

We are IntechOpen, the world's leading publisher of Open Access books Built by scientists, for scientists

6,900

Open access books available

186,000

International authors and editors

200M

Downloads

Our authors are among the

154

Countries delivered to

TOP 1%

most cited scientists

12.2%

Contributors from top 500 universities



WEB OF SCIENCE™

Selection of our books indexed in the Book Citation Index
in Web of Science™ Core Collection (BKCI)

Interested in publishing with us?
Contact book.department@intechopen.com

Numbers displayed above are based on latest data collected.
For more information visit www.intechopen.com



Transient Anions in Radiobiology and Radiotherapy: From Gaseous Biomolecules to Condensed Organic and Biomolecular Solids

Elahe Alizadeh, Sylwia Ptasińska and Léon Sanche

Additional information is available at the end of the chapter

<http://dx.doi.org/10.5772/63293>

Abstract

This chapter focuses on the fundamental processes that govern interactions of low-energy (1–30 eV) electrons with biological systems. These interactions have been investigated in the gas phase and within complex arrangements in the condensed phase. They often lead to the formation of transient molecular anions (TMAs), and their decay by autoionization or dissociation accompanied by bond dissociation. The damage caused to biomolecules via TMAs is emphasized in all sections. Such damage, which depends on a large number of factors, including electron energy, molecular environment, and type of biomolecule, and its physical and chemical interactions with radiosensitizing agents are extensively discussed. A majority of recent findings resulting from experimental and theoretical endeavors are presented. They encompass broad research areas to elucidate important roles of TMAs in irradiated biological systems, from the molecular level to nanoscale cellular dimensions. Fundamental aspects of TMA formation are stressed in this chapter, but many practical applications in a variety of radiation-related fields such as radiobiology and radiotherapy are addressed.

Keywords: ionizing radiation, low-energy electrons, dissociative electron attachment, DNA, strand breaks

1. Introduction

High-energy ionizing radiation (e.g., γ - and X-rays, electrons, and ions) affects biological materials, via a chain of physical, chemical, and biological processes. A complete understand-

ing of these processes in living cells and tissues is a challenging task because of the multiple sequences of events, which lead to cell mutation or death. Nonetheless, such knowledge enhances our ability to cause death or inhibit growth of cancer cells in radiation therapy and to save healthy cells by radiation protection. As shown by many studies [1], cellular deoxyribose nucleic acid (DNA), containing genomic information, is the primary target for cell damage from ionizing radiation. The fundamental mechanisms involved in the induction of damage to DNA by radiation have therefore been subjects of intense investigations during the past decades [2, 3]. When exposed to ionizing radiation, large biomolecules such as DNA and proteins in the cell can be ionized and/or excited. This may effectively cause changes in their molecular structures by inducing bond ruptures and successive fragmentations, which then affect the function and metabolism of the cell. In DNA, the resulting damages may lead to incomplete repair, misrepair, or unrepair of the molecule. The displaced, mismatched, or damaged DNA bases may be misinterpreted during the replication cycle, deterring cell replications and causing accumulation of cancer predispositions for mutations [4–6].

Ionizing radiation damage to DNA can be induced directly by the interactions of primary quanta of radiation via ionization or excitation of individual components of the DNA itself and by secondary particles, including radicals, electrons, and ions generated along the track, after the interaction of primary radiation with molecules surrounding DNA, that is, water and other cellular components [7, 8]. It is by now well established that the consequences of radiation exposure of biological matter at the molecular level are largely due to secondary electrons (SEs), which are formed with a yield of about 5×10^4 per MeV of deposited radiation energy. SEs are the most abundant secondary species generated by the transfer of energy from ionizing radiation into the medium and essentially comprise slow electrons with kinetic energies below 30 eV. The energy distribution of SEs has a most probable energy around 9–10 eV [9], and those electrons of higher initial energy undergo successive energy losses via inelastic collisions, for example, electronic excitation and ionization. These later create further generations of electrons of significantly lower energies. As all electrons necessarily reach the low-energy range ($E < 30$ eV), a detailed knowledge of reactions involving such low-energy electrons (LEEs) with DNA is thus crucial to understand and accurately describe radiobiological damage. LEEs have been shown to induce genotoxic damage, for example, single- and double-strand breaks (SSBs and DSBs) and other multiple damage sites by bond cleavage, chiefly through formation of a transient molecular anion (TMA) of DNA subunit, followed by dissociative electron attachment (DEA) or autoionization of TMA [10].

The main purpose of this chapter is to describe the phenomena related to reactions of LEEs, which may produce biological effects in the cell, such as apoptosis and cell cycle arrest. Since utmost of the harmful mutagenic and lethal damages of ionizing radiation result from chemical modifications in the nucleus of living cells, sustained studies have been focused on the ultrafast mechanisms involved in the direct interaction of LEEs with DNA and its different subunits, as well as indirect processes which are associated to the interactions of electrons with the principal cellular components nearby DNA. An ultimate understanding of LEE damage mechanisms and their role in DNA damage due to radiation can be obtained from experiments with molecular targets of increasing complexity, that is, from simple gaseous and condensed

phase biomolecules to plasmid and cellular DNA. This wide range of target structures is essential to systematically understand how the fundamental principles of the LEE interaction with simple biomolecules and DNA components intervene in more complex ones up to and including cellular DNA [11].

In the first two sections of this chapter, the formation of TMAs and their decay into DEA and autoionization processes are extensively reviewed for simple molecules in the gas and condensed phases. The next section exclusively concerns the interactions of LEEs with basic DNA subunits, that is, the bases, the sugar-phosphate unit, and its two basic constituents in the gas phase. Such studies are necessary to understand how SSBs and DSBs and base release in the much more complex DNA molecule can occur by LEE impact. Additionally, gas-phase DEA to radiosensitizers (halogenated nucleobase, Pt- and nitrogen-based compounds) is discussed in Section 4.

While most of the simple DNA building blocks can be readily vaporized for experimental study to the gas phase, most of the larger units, that is, nucleosides (containing a DNA base + sugar) and entire nucleotides (sugar + base + phosphate group) undergo decomposition during evaporation [12]. Electron attachment to the short oligonucleotides and single-stranded oligomers containing different bases is reviewed in Section 5. Such molecules with a strong tendency to capture electrons and formation of electronically stable anions simplified the analysis of degradation products relative to longer single- and double-stranded configurations [13]. Since histones and the other chromosomal proteins present in the nucleus are in close contact with DNA, reactive species resulting from the interactions of LEEs with nearby amino acids may also interact with DNA, causing indirect damage. There is thus considerable interest in studying the fragmentation of chromosomal proteins induced by LEEs [14], and Section 6 is devoted to the investigations of the action of LEEs on building blocks of proteins, more particularly on amino acids and peptides.

Despite the significance of the gas-phase and condensed-phase experiments in revealing the major interactions of LEE with DNA, the results of these experiments do not essentially correspond to those obtained in the dynamic existent situation of the cell, where cellular DNA lies in a medium containing essentially water with proteins, ions, and vitamins dissolved in the aqueous environment. Section 7 thus reviews recent studies in more complex systems, where a DNA molecule is embedded into more realistic environments containing water, oxygen, histones, and DNA-binding proteins that mimic cellular conditions.

The role of secondary LEEs in radiosensitization and radiation therapy is discussed in the final section of this chapter. LEEs have subcellular ranges (on the order of 10 nm) in biological materials and interact strongly and destructively with chemical bonds; so, they are ideal for promoting local (i.e., nanoscopic) increases of radiation damage in cells, particularly for targeted cancer therapies. We review a wealth of experimental data on LEE-induced lesions in DNA bound to radiosensitizing gold nanoparticles and the platinum-chemotherapeutic agents. This final section links the effects of radiation and chemotherapy, showing that by modulating the radiation chemistry, chemotherapeutic agents can become radiosensitizers. It also explains how our fundamental understanding of LEE-induced DNA damage can be

applied to optimize concomitant chemoradiation therapy (CRT) by modifying the action of LEEs or by increasing their numbers in cancer cells.

2. Decay of Gaseous Transient Anions into Dissociative Electron Attachment (DEA) and Autoionization

In electron–molecule collisions, a TMA is formed, when an incoming electron occupies a previously unfilled orbital of a molecule for duration greater than the usual scattering time [15–17]. Since such an orbital exists at a precise energy [15], TMAs are formed at specific energies usually below 15 eV and rarely above 30 eV [15, 16]. Because of the uncertainty principle, the transient state has a width in energy, which characterizes and identifies the process in the dependence on incident electron energy of cross sections for particular energy-loss processes or the formation of the products or damage yields (i.e., the yield functions). Thus, at the resonance energy, corresponding to the formation of the TMA, yield functions exhibit pronounced maxima that can be superimposed on monotonically increasing background, which results from nonresonant or direct scattering.

The formation of TMAs is well described and reviewed in the literature [15–21]. There are two major types of TMAs or “resonances” [15–17]. The first, known as a single-particle resonance, occurs when the additional electron occupies a previously unfilled orbital of a molecule (or subunit of a large biomolecule) in its ground state. Here, the electron is temporarily trapped within an angular momentum barrier by the shape of the electron–molecule potential. Such TMAs are thus also termed shape resonances. Core-excited resonances or “two-particle, one-hole” states form when electron capture is accompanied by electronic excitation, such that two electrons occupy previously unfilled orbitals. The incident electron is in effect captured by the positive electron affinity of an excited state of the molecule or basic subunit in the case of a large biomolecule, which for DNA might include a base, sugar, or phosphate group. If a momentum barrier in the electron–molecule or electron-subunit potential contributes to the retention of the electron in the electronically excited molecule or subunit, the transitory anion is referred to as core-excited shape resonance. If the TMA state is dissociative and the resonance lifetime is greater than about half of the vibration period of the anion, the latter dissociates. This process is called DEA.

The decay of a TMA into dissociative channels can be understood by considering the hypothetical internuclear potential-energy curve of a diatomic molecule AB and one of its TMA state AB^- shown in **Figure 1**. While the following description is rigorously applicable only to diatomic molecules, it is still qualitatively valid along a specific bond of a polyatomic molecule. Assuming that only Franck–Condon (F–C) transitions are possible and that the AB^- state is dissociative, we see from the consideration of the ground-state nuclear wave function that electrons with energies of between E_1 and E_2 are required to fragment AB^- . However, its fragmentation into $A^- + B$ is only possible if its life time is long enough to survive autodetachment, which can occur for internuclear separations, $R < R_C$. For $R > R_C$, AB^- is stable against autodetachment, as electron emission is endothermic. If the TMA does not dissociate, the

electron is re-emitted into the continuum, leaving the target in vibrational, rotational, or even electronically excited states in the case of a core-excited TMA.

When the TMA state lies above the electronically excited states of the molecule, this later can acquire electronic energy, after autoionization of the anion, in addition to vibrational and rotational motion. If the electronic excited state is dissociative, then fragments A and B (Figure 1) are produced. Thus, both decay by autoionization into dissociative electronically excited states and DEA cause the molecule to fragment.

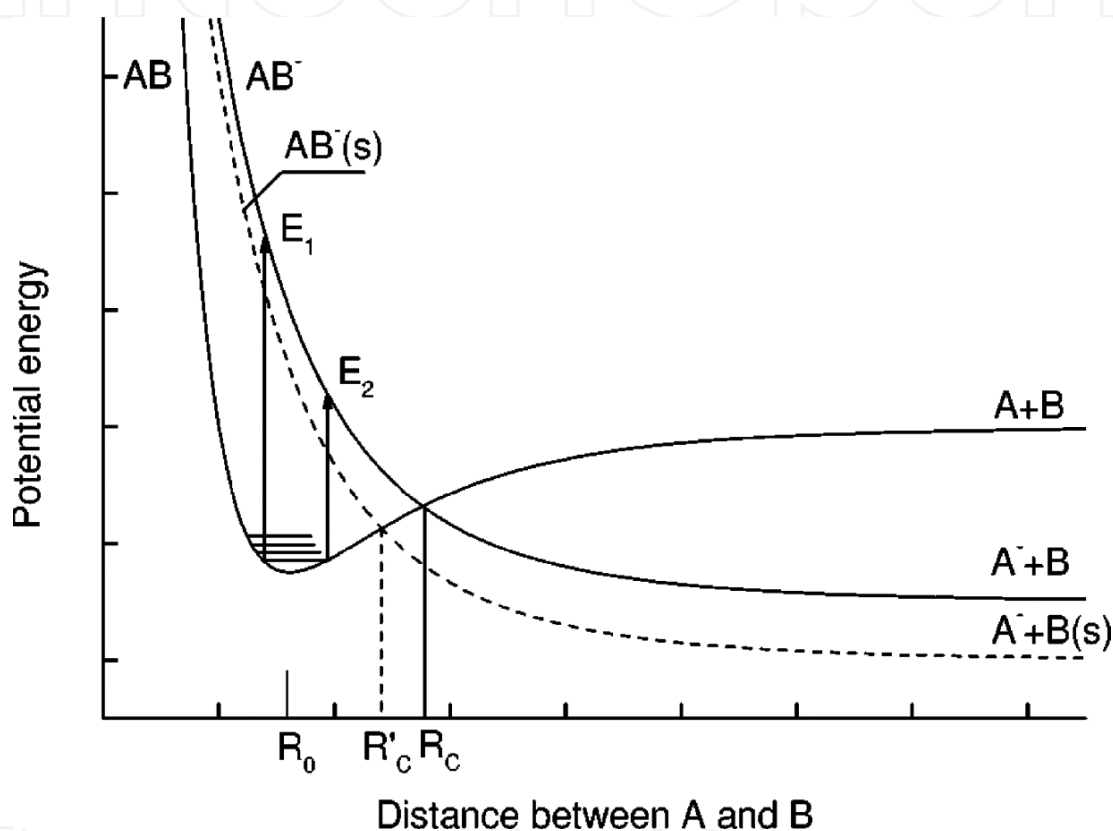


Figure 1. Born–Oppenheimer potential-energy curves associated with dissociative electron attachment. AB represents the potential-energy curve of the ground state of a diatomic molecule and AB⁻ represents a dissociative state of a corresponding transient anion. The dashed line, AB⁻(s), represents the potential-energy curve of AB⁻ within a molecular solid. R_0 is the equilibrium distance between A and B in the ground-state AB. AB⁻ is stable against autoionization for $R > R_c$.

Within a local complex potential–curve–crossing model, the DEA cross section may be expressed as

$$\sigma_{DEA}(E) = \sigma_{CAP} \cdot P_s \quad (1)$$

where P_s represents the survival probability of the anion against autodetachment of the electron. The capture cross section σ_{CAP} is given by:

$$\sigma_{CAP}(E) = \lambda_e g |\chi_v|^2 \left[\frac{\tilde{A}_a}{\tilde{A}_b} \right] \quad (2)$$

where λ_e is the de Broglie wavelength of the incident electron, g is a statistical factor, and χ_v is the normalized vibrational nuclear wave function. Γ_a and Γ_b are the local energy widths of the AB^- state in the F–C region and the extent of the AB^- curve in the F–C region, respectively. The width of the transient anion state in the autodetaching region defines the lifetime τ_a toward autodetachment, $\tau_a(R) = \hbar / \Gamma_a(R)$, such that the survival probability of the TMA, after electron capture, is given by

$$P_s = \exp \left[- \int_{R_0}^{R_c} \frac{dt}{\tilde{A}_a(R)} \right] \quad (3)$$

where R_0 is the equilibrium bond length of the anion at energy E and R_c is the internuclear separation beyond which autodetachment is no longer possible. Hence, the DEA cross section depends exponentially on the lifetime of the TMA and the velocities of the fragments.

For further information on the mechanism of TMA formation and its effects on isolated electron–molecule systems, the reader is referred to previous works [15, 16, 22–26]. Information on resonance scattering from single layer and submonolayers of molecules physisorbed or chemisorbed on conductive surfaces can be found in the review by Palmer and Rous [20]. The following section provides information essentially on TMA formation in the condensed phase (i.e., in molecules in solids, condensed onto a dielectric surface or forming a molecular or biomolecular thin film).

3. Modification of electron capture and decay of transient anions in the condensed phase

In principle, the formation and decay of TMAs of condensed molecules can be described using a modified gas-phase picture. For molecular solids or sufficiently thick molecular films condensed onto a metallic substrate or a dielectric surface, the target molecules are unaffected by the substrate, and they exist in the physisorbed state [27]. This weak form of adsorption is characterized by a lack of a chemical bond between molecules, so that the electronic structure and vibrational frequencies of the condensed molecule are essentially unchanged from those in the gas phase [17, 27]. Conversely, electron–molecule scattering is modified in the condensed phase as well as the properties of TMAs [17, 20].

Low-energy (0 – 30 eV) electrons have wavelengths comparable to the distance between molecules in condensed media. Hence, they interact within molecular solids via delocalized processes, predominantly including static and correlation interactions with neighboring molecules, excitation transfer, and coherent scattering [28–31]. Such conditions make it difficult

to transfer electron scattering and attachment data from the gas phase to the condensed phase. Even though theoretical models have tried to approximate these processes, the resulting calculations differ substantially from the available experimental data [31–34]. For example, in the gas phase, the incoming electron wave function is a plane wave, whereas scattering events in the condensed phase are those of a diffracted electron wave function that depends on the ordering of the solid. It can be readily seen from Eq. (2) that this change in the partial wave content of the scattered electron wave modifies the capture cross section. Furthermore, Γ_a in Eq. (2) changes in the condensed phase, since new decay channels (e.g., phonon modes) appear and the TMA is formed at lower energy due to the polarization potential induced by the temporarily localized electron [17, 35] and possible lowering of the symmetry of the anion state [20]. The dash curve in **Figure 1** shows the lower energy of the potential-energy curve of the condensed-phase transient anion AB^- . The lower energy causes the curves AB and AB^- to cross at a shorter internuclear distance R_C' than that in the gas phase (R_C). This leaves less time for autoionization of the TMA. In other words, the value of the integral in Eq. (3) becomes smaller, and P_s becomes larger. Moreover, lowering the potential curve of the TMA changes the number of decay channels. The intramolecular channels are decreased because of the lower TMA energy, but new intermolecular channels must be added to take into account decay into collective vibrations (phonon modes). Hence, the resonance lifetime may increase or decrease, and so the DEA cross section (i.e., the DEA intensity depends on the details of AB and AB^- potential-energy curves and the number of decay channels). In addition, electron transfer from one molecule to another may occur, and hence provide additional decay pathways for TMAs [36]. For very large biomolecules, such as DNA, electron transfer between elemental subunits also impedes electron localization [35]. Hence, due to intramolecular electron transfer, the probability of TMAs forming on specific subunits can also be reduced.

The increase in DEA cross section resulting from the shift of the curve crossing point in **Figure 1** from R_C to R_C' can be illustrated experimentally by covering a metal surface with a multilayer film of a condensed rare gas and depositing a molecule on the film surface. As an example, **Figure 2** shows the result of such an experiment in which a 0.1 monolayer (ML) of CH_3Cl was condensed onto a 20 ML thick Kr film [37]. The variation of a surface charging coefficient A_s , which is directly proportional to the absolute cross section (μ) for the reaction (1) recorded between incident electron energies 0 and 2.5 eV, is shown in the inset of **Figure 2**.



Within this energy range there exists a single structure in the A_s energy dependence, the maximum of which lies at approximately 0.5 eV for large Kr coverage. The peak denotes the energy of the TMA CH_3Cl^- . As the Kr film thickness is reduced, the transitory CH_3Cl^- anion moves closer to the metal substrate, and the energy of the maximum in the inset lowers owing to the larger polarizability of the metal compared to Kr. The lower curve in **Figure 2** shows this shift in energy of CH_3Cl^- with decreasing thickness. However, as the energy of transitory CH_3Cl^- on the Kr film lowers, according to **Figure 1**, R_C' becomes smaller and P_s increases. Thus, as seen in the experimental curve with the full squares in **Figure 2**, the magnitude of the

absolute cross section for Cl^- production at the peak values increases with decreasing thickness of the Kr film. When CH_3Cl^- is formed too close to the metal substrate, the additional electron transfers to the metal, and μ sharply decreases.

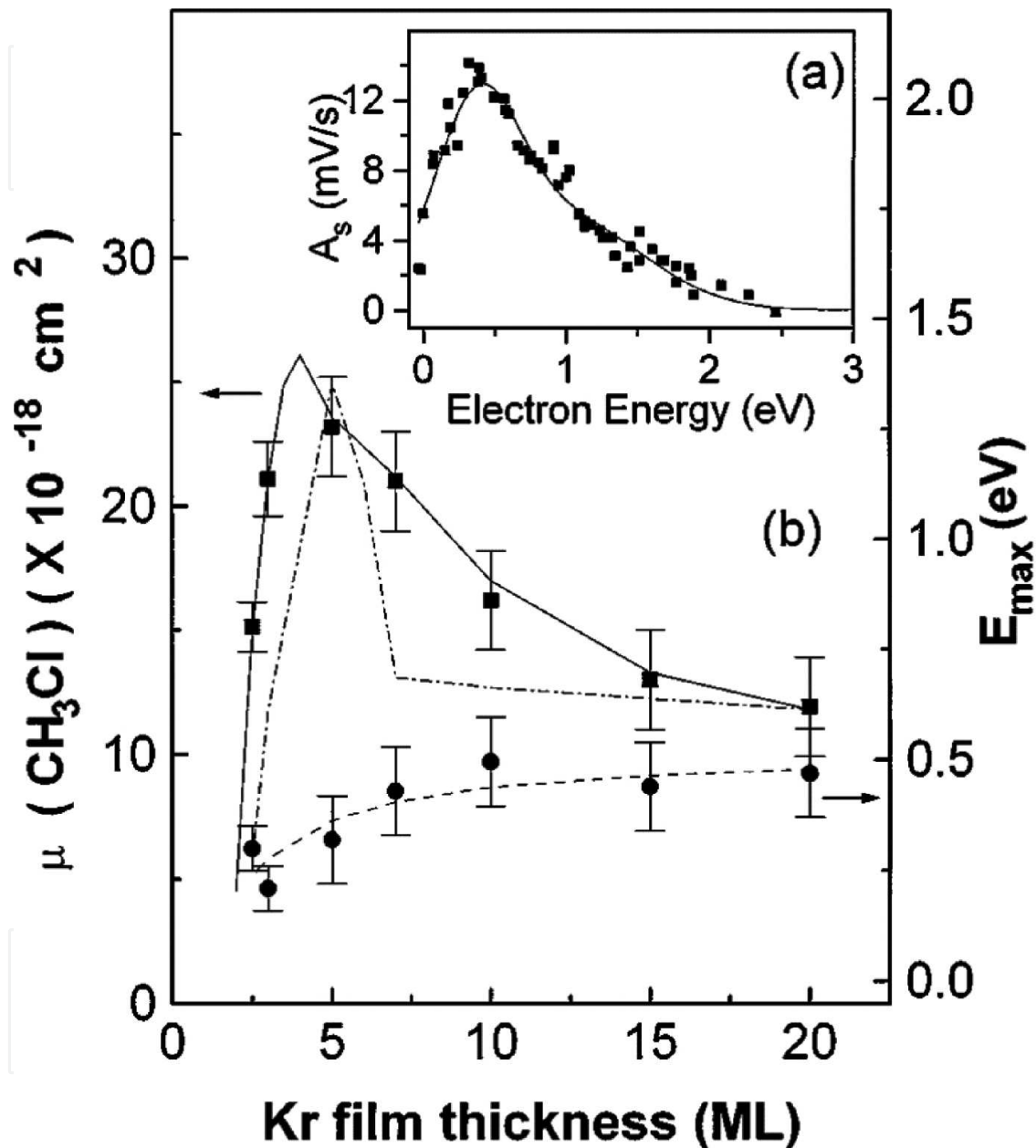


Figure 2. CH_3Cl^- formation and dissociation by electrons of 0–2.5 eV incident on submonolayer amounts of CH_3Cl physisorbed on a multilayer film of Kr. (a) Variation of the charging coefficient of the film A_s due to CH_3Cl^- dissociation. (b) Variation with film thickness of: (■) the amplitude of the maximum in the charging cross section (μ); (•) the amplitude of the maximum in μ calculated with the *R*-matrix method [37]; (•) variation of the energy of maximum in μ and A_s ; and (---) a parametric fit of this maximum using the image charge model [38].

In the condensed phase, TMAs differ from their gas-phase counterparts, in the following ways: (1) the electron energies required for their formation are usually lower by 0.5–1.5 eV, dependent

on the local polarization of the solid and/or changes to the anion's symmetry; (2) due to their lower energies, they usually have fewer intramolecular decay channels, although, new intermolecular channels via electron emission into the dielectric may appear; (3) the lifetimes will be longer or shorter due to the changes in the number of decay channels, energy, and symmetry; (4) the initial electron capture probability, and the cross sections for decay into particular intermolecular and intramolecular excitations or for DEA may vary by orders of magnitude, as these are dependent on energy, intramolecular and intermolecular electron transfer, and symmetry. In summary, when a TMA is formed on a molecule located inside or at the surface of a molecular or biomolecular solid, its gas-phase characteristics are usually considerably affected by the local environment.

4. DEA to gaseous DNA subunits and radiosensitizers

4.1. DNA bases

A large number of DEA studies have been performed on gas-phase DNA bases and their derivatives over the last two decades [2, 39]. Briefly, DEA is the resonant process that involves the LEE capture by a molecule (AB) to produce gaseous TMAs ($(AB)^-$), described in Section 2, which then dissociate into an anion (A^-) and a neutral radical or radicals (B^\bullet), according to the following reaction:



In general, the low-energy resonances in nucleobases are present either at subexcitation (< 3 eV) energies or in the energy range 5–12 eV [39]. The yield function for the DEA processes for thymine resulting in multiple fragment formation is shown in **Figure 3**. To analyze the formation of the negative ions, yield functions were usually recorded by scanning the incident electron energy, while potential voltages applied to the quadrupole mass spectrometer were set for a given ion mass. The ion yields were detected by a channeltron and plotted as a function of the incident electron energy.

The high-energy resonances lead to transient anion fragmentation via opening of the ring structure, while the low-energy resonances are primarily due to loss of one or two neutral hydrogen, which maintains the ring structure.

The DEA yield functions for nucleobases and their related compounds show a remarkable feature that can be recognized as a common phenomenon, that is, site selectivity [40–42]. By tuning the energy of the incoming electron, it is possible to control the location of the bond cleavage. That is, a specific chemical bond in a molecule can be targeted by electrons followed by fragmentation. As an illustration of this site selectivity in nucleobases, DEA to thymine with deuterated and methylated substitutions is described. This phenomenon was observed for other nucleobases and their derivatives, for example, adenine [43] and hypoxanthine [44].

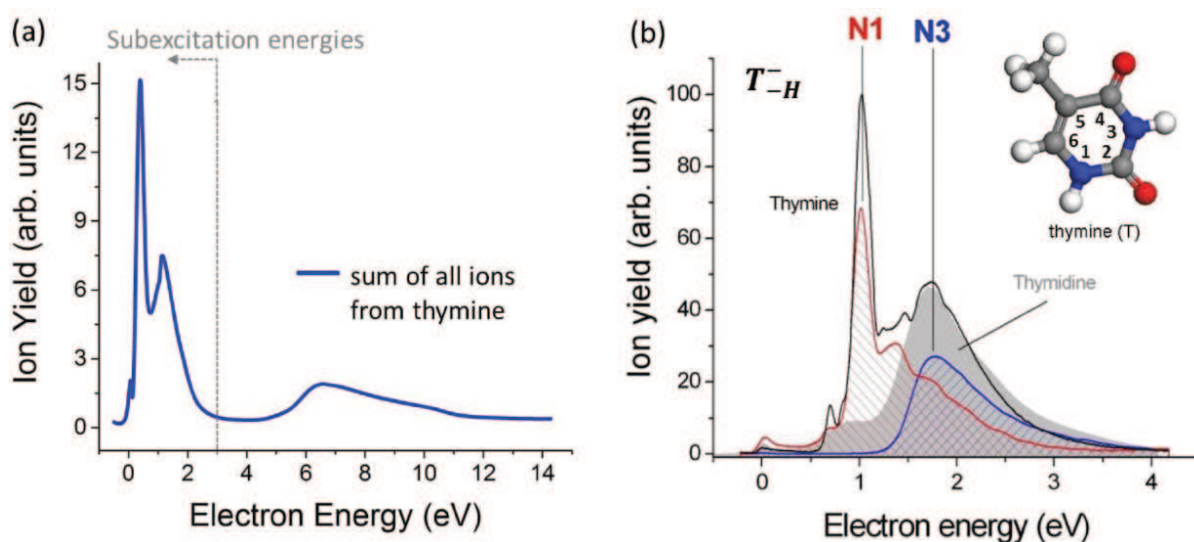


Figure 3. (a) Total ion yield as a function of electron energy for DEA process of thymine. (b) Formation of dehydrogenated anions from thymine (black curve), methylated thymine at N3 site (red curve), methylated thymine at N1 site (blue curve), and thymidine (gray area) [45]. Molecular structure of thymine with numbering and atom labeling.

At subexcitation energies, DEA leads to thymine dehydrogenation by loss of a neutral hydrogen atom [40, 42]. This reaction can be expressed as follows:



where T^- is the TMA of thymine (T) and T_{-H}^- is the closed-shell anion formed by the ejection of a neutral hydrogen radical $\langle i \rangle H^\bullet \langle /i \rangle$. This dehydrogenation process depends on the site from which the H atom is removed. Experimental studies with partially deuterated thymine, in which the deuterium is at either nitrogen or carbon sites, showed that hydrogen loss occurs exclusively from the N sites. H loss from the C sites is thermodynamically accessible within this energy range, but has not been observed experimentally. Moreover, in employing methylated thymine and uracil, it has been shown that by adjusting the electron energy, the loss of H can be made even site-selective with respect to the N1 and N3 positions. Although 1 eV electrons induce H loss at the N1 position (N1-H), the process can be switched at 1.8 eV to N3-H (**Figure 3b**). These results have significant consequences for the molecular mechanism of DNA strand breaks induced by LEEs. Within DNA, the N1 position of thymine is coupled with the sugar moiety and thus forms thymidine, which is one of the nucleosides. Because the shapes of the signals from thymine and the more complex thymidine resemble each other, it can be concluded that H abstraction in thymidine predominantly occurs at the thymine moiety and, more precisely, at the N3 position (**Figure 3b**) [45].

In addition to the detection of anions and the energies at which they are formed, much effort has been expended to matching particular types of DEA process to specific resonant peaks observed in DEA ion yields. In the case of the most abundant anion formed for all nucleobases,

it has been proposed that these resonant peaks can be assigned to vibrational Feshbach resonances (VFRs) [46, 47]. VFRs usually occur at low energies, when vibrational levels of the transient anion lie below the corresponding vibrational states of the neutral, and are more expected in greatly polarized molecules with very large dipole moment, which leads to a long-range attractive interaction. They may serve as a gateway for dissociation at low energies if they are coupled with a dissociative valence state. This can be the case for the formation of dehydrogenated ions from nucleobases, where resonances arise from coupling between the dipole bound state and the transient anion state associated with the occupation of the lowest σ^* orbital. Recently, the nucleobase fragmentation of N–H bonds induced by LEEs was studied by employing the CASPT2//CASSCF computational approach [48]. These calculations showed that the two lowest lying π^* states can be determined at energies below 1.0 eV and above 2.0 eV for pyrimidines, whereas for purines, this energy gap between the two anionic states was less pronounced. These calculations also suggested the possibility of coexistence of dipole-bound and valence-bound processes in the low-electron energy range.

Further to the observations of site selectivity in DEA processes leading to single-bond cleavage within a nucleobase, site selectivity also occurred in multiple-bond cleavage. As in the cases of both dehydrogenation of nucleobases and its complementary channels, which resulted in the H^- formation, site selectivity was demonstrated when multiple-bond cleavage was involved, for example, for the formation of NCO^- from thymine and its derivatives [49]. This anionic fragment was formed in a sequential decay reaction, in which the dehydrogenated anionic nucleobase acts as an intermediate product. In this case, the remarkable resonances, which were observed for dehydrogenation and for H reaction channels in nucleobases, were preserved for the subsequent decay reaction, leading to the formation of NCO^- as the final product.

In general, the total cross sections for DEA to nucleobases exhibited comparable magnitudes in the energy range for TMA formation [50]. However, these cross sections were up to 10 times smaller than those for the formation of single-strand breaks, while the cross sections for sugar and phosphate group analogs (see Section 4.2) were even smaller in magnitude.

4.2. Sugar and phosphate group

The high fragility of the DNA backbone with respect to the impact of LEEs with low kinetic energy was observed for 2-deoxy-D-ribose and its RNA equivalent (i.e., ribose), along with their analogs [2]. In principle, the dissociation of any of P–O–C bonds in the sugar–phosphate backbone or C–C bond within the sugar could result in a DNA strand break. If such breakages were to occur via the DEA process in DNA, then DEA would represent an important pathway through which the direct interaction of LEEs could affect biologically significant damage.

The DEA to 2-deoxy-D-ribose results in a strong decomposition of the sugar at electron energies near 0 eV, indicating the loss of one or more molecules of water [51]. Similar findings were observed for D-ribose and other sugars [2], indicating that DEA at 0 eV is a common property of all monosaccharides. However, the mechanisms for DEA reactions leading to loss of neutral water are more complex in comparison to the dehydrogenation of the nucleobases, because they involve the dissociation of multiple bonds and/or atom rearrangement with

simultaneous formation of new bonds. Therefore, the mechanism of DEA to sugars near 0 eV is not fully understood. It is however proposed to occur via the formation of a “shape” resonance. In a sugar molecule, the extra orbital can be a σ^* orbital of the O–H bond. As was observed for alcohols [52], the σ^* orbital of the hydroxyl group for the dehydrogenation channels appears at higher energy for simple alcohols than for cyclic alcohols. Moreover, it was found that larger numbers of hydroxyl groups present in a molecule could enhance the dissociation of an O–H bond, by decreasing the energy of the thermodynamic threshold. This mechanism has been suggested for 2-deoxy-D-ribose and D-ribose, which contain three and four hydroxyl groups, respectively [2]. In addition, experiments with the ribose analogs tetrahydrofuran and 3-hydroxytetrahydrofuran showed that DEA cross sections were greatly enhanced by the presence of OH groups [50]. However, for alcohols, their molecular dissociation involved simple bond cleavage, while in sugars, fragmentation of several different bonds occurs. One of the proposed models for sugar dissociation was provided from ab initio calculations of VFRs formed initially by a dipole-bound state of sugar due to a large dipole moment [53]. Other quantum chemical calculations confirmed this model, showing that the sugar ring can convert into an open chain by intramolecular charge transfer. This mechanism can lead to dissociation by loss of a water molecule, assuming that the barrier for such a transfer is sufficiently low [54]. It was also calculated through quantum dynamics scattering theory that the formation of shape resonances for D-ribose is excluded at low energies, but they can be formed at higher energies [55].

In the case of thymidine, in which sugar is covalently bound to thymine, the DEA study showed two resonant structures (**Figure 3b**) [45]. The one at lower energy was associated with a reaction in which the excess electron is initially localized in the sugar moiety, leading to the glycosidic bond cleavage. The second resonance was attributed to a reaction in which the excess electron was localized on the thymine moiety, resulting in the loss of a neutral H atom from the N3 site, as was mentioned for thymine. Since nucleosides can be easily decomposed due to the elevated temperatures necessary for evaporating samples, no experimental data for other gas-phase nucleosides or nucleotides are reported, besides those for thymidine [45], cytidine [56], and 2-deoxycytidine 5-monophosphate [56].

Similarly, due to experimental difficulties, the phosphate group in the gas phase could not easily be investigated as an isolated compound. Its simplest analog, H_3PO_4 (phosphoric acid), is not easily vaporized for gas-phase experiments or molecular deposition for thin film experiments [11]. Therefore, to understand the DEA process within the phosphate group, several compounds involving phosphoric acid derivatives, for example, dibutylphosphate and triethylphosphate [57], were examined. DEA to these compounds lead to P–O and C–O bond cleavages, which correspond to a direct single-strand break. As for sugars, many fragmentation channels occurred close to 0 eV; however, these low-energy channels are most likely driven by the large electron affinity of PO_3 (4.95 eV). The cross sections for DEA to the sugar and phosphate group analogs were relatively small, that is, about one magnitude lower than those for nucleobases [50]. These gas-phase results on sugars and phosphate units revealed that LEE attachment can induce single-strand breaks by electron localization either on the sugar moiety followed by the electron transfer to the backbone or directly on the phosphate group.

4.3. Radiosensitizers

An important characteristic of many current and potential radiosensitizers used in radiotherapy (or potential ones) is a high cross section for DEA. Since halogenated pyrimidines, mainly substituted uracil derivatives, exhibit high sensitivity to electron attachment and a rich fragmentation pattern from DEA, they have attracted considerable interest as radiosensitizers. From a medical point of view, the substitution of pyrimidines in the genetic sequence of cellular DNA does not affect the gene expression, and additionally enhances the sensitivity of living cells to radiation. A large number of gas-phase experimental and theoretical studies of several halogenated pyrimidines (e.g., 5-bromouracil [58–63], 5-chlorouracil [58, 59, 61, 64, 65], 5-fluorouracil [58, 59, 61, 65], 5-iodouracil [59, 62], 6-chlorouracil [58,66]) were performed in recent years and report orders of magnitude of higher cross sections for DEA relative to their nonsubstituted precursors. Further to the DEA studies, other electron spectroscopic techniques and theoretical calculations at the *ab initio* and density functional theory levels were utilized to characterize electronic structure and reveal the fragmentation mechanisms of halogenated pyrimidines [67]. These studies elucidated the energies of vertical transitions to π^* and σ^* orbitals, showing that the ground TMA state of pyrimidine with the additional π^* electron is a few tens of eV more unstable than the neutral ground state, whereas the vertical electron affinities of the halogenated derivatives were found to lie close to 0 eV. Moreover, DEA studies revealed that the lowest π^* anion states of the halogenated pyrimidines follow similar fragmentation channels, resulting in the formation of the halide fragment anion. These studies also revealed that the total anion yields for bromopyrimidine were much larger than those measured for the chloro-derivatives. These results indicate that bromopyrimidines carry the greatest potential as radiosensitizers for damage by SEs, which, via DEA to bromo-substituted DNA, will enhance radiation-induced damage to the cell. Recently, gas-phase DEA studies on halogenated purines (e.g., chloroadenine [68]) and fluorinated nucleosides (2-deoxy-5-fluorocytidine and 2,2-difluorocytidine (gemcitabine) [69]) have been initiated to determine in what ways their radiosensitizing properties are derived from LEE-driven chemistry.

In addition to the halogenated nucleobases, several aromatic compounds containing nitro groups have been recently investigated in the gas phase. For instance, DEA studies performed for 5-nitrouracil showed the formation of a long-lived parent anion, as well as a rich fragmentation pattern via formation of either “shape” or “core-excited” resonances at low electron energies [70, 71]. The properties of 5-nitrouracil showed a radiosensitizing nature similar to that of the halogenated pyrimidines. Interestingly, while in the case of halogenated pyrimidines, the most dominant fragment formed was a halide anion, that for 5-nitrouracil is an anion of the pyrimidine without a nitro group. Therefore, the counterpart fragment of this dissociation channel is the formation of the NO_2 radical, which is formed in close vicinity to DNA and can lead to the activation of lethal cluster damage in living cells.

There is also a great potential for other nitro-containing compounds such as nitroimidazolic compounds to be used in radiotherapy, since LEEs effectively induce their dissociation [72, 73]. Similarly, their decomposition via DEA involves a range of unimolecular fragmentation channels from single-bond cleavages to complex reactions, possibly leading to a complete degradation of the target molecule. However, these studies revealed that the entire rich

chemistry induced by DEA was completely suppressed by methylation in the electron energy range below 2 eV.

In recent years, platinum-based drugs were also investigated regarding their decomposition by LEEs. It was suggested that in concomitant treatment in which chemotherapeutic drugs and radiotherapy are combined, one possible mechanism responsible for the observed synergy between treatments is the enhancement in the number of secondary species induced by primary radiation in the vicinity of the binding site of the platinum compounds in DNA (see Section 8). The gas-phase DEA studies of PtBr₂ in the electron energy range between 0 and 10 eV showed the formation of the Br anion via two possible channels. The most dominant channels were assigned to the Br⁻ + PtBr dissociation limit reached at ~1 eV and the higher energy channel to Br⁻ + Pt + Br [74].

The observation that all these radiosensitizers exhibit DEA with high efficiency, even close to 0 eV, may have significant implications for the development and use of these drugs in tumor radiation therapy. Considering their use as radiosensitizers, their fragmentation and the resulting generation of radicals at very low electron energies may be a key in understanding their action and the molecular mechanisms necessary to improve radiotherapy.

5. Electron attachment to short single-stranded and plasmid DNA

Cellular DNA consists of a double-stranded helical structure, composed of two long polynucleotide chains [75]. Thus, as already mentioned in the Introduction section, in order to systematically understand LEE damage mechanisms and their role in radiation DNA damage, molecular targets of increasing complexity were studied, from simple molecules containing just two of the basic subunits (e.g., a phosphate group coupled with a sugar or a nucleoside having a DNA base + sugar), via synthetic, single- and double-stranded oligonucleotides, containing multiple nucleotides to plasmid and other cellular DNA with many thousands of base pairs.

Even though most simple DNA components may be easily vaporized for experimental investigation in the gas phase, the larger units such as nucleosides and nucleotides usually decompose during evaporation [12]. In any case, the condensed phase is certainly the more appropriate environment to study problems relevant to radiation damage in biomolecular systems. The experimental methods and techniques, used in the condensed phase, differ from those in the gas phase. Most condensed phase experiments are achieved by bombarding thin films (2–10 nm) of oligonucleotides or plasmid DNA with an energy-selected beam of LEEs from an electron gun or an electron monochromator. To prevent excessive charging, these thin-film biological samples are deposited onto a metal substrate by spin-coating, lyophilisation (freeze-drying), or molecular self-assembly, as in the case of thiolated DNA on gold substrates [10] and 1,3-diaminopropane layer plasmid on graphite [76]. The LEE-induced damage to plasmid and linear DNA films has then been investigated by (1) measuring electron-stimulated desorption (ESD) of anions, (2) imaging the breaks by atomic force and scanning tunneling microscopies, and (3) analyzing, after bombardment, the change of DNA topology by gel

electrophoresis or the molecular content by high-performance liquid chromatography (HPLC) and mass spectroscopy [35, 77].

Oligomers of single-stranded DNA containing the four bases (e.g., G, C, A, and T), which are among the simplest forms of DNA, have made the analysis of degradation products much simpler than would be the case for longer single- and double-stranded configurations. Short oligomers deposited onto metal surfaces (e.g., tantalum, platinum, and gold) as films of different thicknesses (1–5 ML) were bombarded with LEEs and produced fragments analyzed by HPLC [77]. The results for the GCAT oligonucleotide indicated that strand breaks occur preferentially by cleavage of the C–O bond rather than the P–O bond, with two maxima at electron energies of 6 and 10 eV [78, 79].

Recently, Bald and co-workers demonstrated the visualization of LEE-induced bond cleavage in DNA origami-based DNA nanoarrays on the single-molecule level using atomic force microscopy (AFM) [80–82]. This novel method has a number of advantages: (1) only miniscule amounts of material are required to create submonolayer surface coverage, because of the facility to detect the DNA strand breaks at a single-molecule level; (2) within a single experiment, more than one oligonucleotide sequence with various arrangements can be irradiated to efficiently compare a number of different DNA structures; (3) the method represents a simple way to obtain absolute strand break cross sections, thus providing benchmark values for further experimental and theoretical studies, and finally (4) this technique is not limited to single strands, but can be extended to quantify DSBs and to investigate higher order DNA structures.

Applying this technique, Bald and coworkers compared the absolute strand break cross sections of different 13-mer oligonucleotide sequences (i.e., 5'-TT(XTX)3TT, with X = A, C, or G) to evaluate the role of the different DNA nucleobases in DNA strand breakage. They also studied the sensitizing effect of incorporation of 5-bromouracil (BrU) by comparing the absolute strand break cross sections for the sequences 5'-TT(XBrUX)3TT, with X = A, C, or G. The observed trend in the absolute strand break cross sections agrees qualitatively with the previous HPLC studies investigating the fragmentation of oligonucleotide trimers of the sequence TXT, with X = A, C, G, irradiated with 10 eV electrons [83]. Additionally, the cross sections measured with this method are comparable in magnitude with the cross sections for strand breaks in different plasmid DNA molecules induced by 1–10 eV electrons, as determined by agarose gel electrophoresis [84, 85]. The DNA nanoarray technique thus bridges the gap between very large genomic double-stranded DNA and very short oligonucleotides, and enables the detailed investigation of sequence-dependent processes in DNA radiation damage. Further experimental and theoretical studies are carried out covering a broad range of electron energies and DNA sequences to elucidate the most relevant damage mechanisms [86].

In order to increase the complexity of targeted biomolecules, several studies have investigated the damage induced by LEEs in double-stranded plasmid DNA. Due to the supercoiled arrangement of plasmid DNA, a single-bond rupture in a DNA with a few thousand base pairs can produce a conformational change in the topology of the entire molecule. These changes include base alterations, abasic sites, intra- and inter-strand base cross-links, DNA adducts, and SSBs or DSBs; hence, these can be detected efficiently by techniques such as gel electro-

phoresis. This technique can identify supercoiled (SC), nicked circular (C), full-length linear (L), cross-linked (CL), and short linear forms of DNA, which can be assigned to undamaged DNA, SSBs, DSBs, several types of cross-linked DNA, and multiple double-strand breaks (MDSBs), respectively [87].

Though it has been established that most of the strand breaks induced by ionizing radiation have been repaired by a DNA ligation step, a DSB represents a particularly detrimental lesion that poses a serious threat to the cell, since it usually cannot be easily repaired [88]. Indeed, even a single DSB can lead to cell death if left unrepaired or, more worryingly, it can cause mutagenesis and cancer if repaired improperly [89].

The results obtained for LEE-irradiated supercoiled plasmid DNA in several investigations are well described in the literature and summarized in authoritative review articles [10, 11, 35]. These studies have shown that SSBs can occur as a result of DEA at electron energies well below electronic excitation and ionization thresholds (0.8–10 eV) [83, 90]. The results of Martin et al. [90] reveal two resonant peaks at 0.8 and 2.2 eV in the SSB yield function (i.e., the number of strand breaks versus the incident electron energy) via the formation of TMAs. These findings are consistent with theoretical calculations indicating that SSBs induced by near-zero energy electrons are thermodynamically feasible [91–93]. Theoretical simulations of electron scattering and electron capture via “shape” resonances support the role of LEEs in DNA strand breaks [94]. Theoretical calculations on scattering and attachment of LEEs to DNA components up to supercoiled plasmid DNA have been intensively reviewed in recent years [95, 96].

Another spatially resolved technique that exploits the use of graphene-coated Au thin films and surface-enhanced Raman spectroscopy (SERS) has recently emerged. Utilizing this technique, the sequence dependence of DNA damage at excitation energies < 5 eV can be studied [97]. Currently, Ptasińska and coworkers are performing a quantitative and qualitative investigation of the various types of damages to dry and hydrated DNA induced by exposure to helium and nitrogen atmospheric pressure plasma jets (APPJs). Since an APPJ contains multiple reactive species, including LEEs, also found in radiation chemistry, exposure to these plasma jets provides information on both the direct and indirect pathways to damaging DNA. Ptasińska and coworkers have employed nitrogen APPJ to induce DNA damage in SCC-25 oral cancer cells, and have thus provided new insight into radiation damage to a cellular system [98].

6. LEEs interaction with protein building blocks

It is well known that within the cells, DNA is in close contact with, and packed by, chromosomal proteins (histones). The attachment of proteins protects DNA from damage by compaction (e.g., which restricts easy access by free radicals to DNA) and repairs some of the damage of electron/hydrogen donation [99]. LEE damage to proteins within cells should not, by itself, cause significant long-term biological damages, because proteins can be replaced. However, due to the presence of histones and other chromosomal proteins in the vicinity of DNA, reactive species produced from LEE interactions with protein constituents (e.g., nearby

amino acids) may in turn interact with DNA, causing indirect damage. Thus, from a radiobiological point of view, there is considerable interest in studying the action of LEEs on this important class of biomolecules [100]. Recent work has focused on the building blocks of proteins, that is, amino acids and small peptides, since the size and complexity of chromosomal proteins prevent direct detailed analysis of the fragmentation processes induced by LEEs [11, 39]. Indeed, measuring the fragmentation of amino acids and their analogs is no more complex than it is for DNA constituents (see Sections 4 and 5) [101–103], and can help elucidate the effects of electron irradiation in larger more complex proteins [103].

In the recent years, several investigations have employed soft ionization techniques, such as matrix-assisted laser desorption ionization (MALDI) [104–107], electrospray ionization (ESI) [108, 109], and collision-induced dissociation (CID) [110–114], to study the ionization and fragmentation of different amino acids and small peptides in the gas phase. Gas-phase investigations of LEE-induced damage to protein subunits have been reported for the amino acids alanine [115], tyrosine [116], glycine [117, 118], proline [119, 120], cysteine [121], and serine [122, 123], as well as small peptides, such as dialanine [124] and amino acid esters [125]. For all cases, the anion yield functions (i.e., ion yields measured as a function of electron energy) exhibited localized maxima at energies below 15 eV, indicating the formation of TMAs. It has been established that no intact parent anion is observable on mass spectrometric timescales after capture of a free electron, and that the most probable reaction corresponds to the loss of a hydrogen atom from a carboxyl group to form for a molecule “M,” the dehydrogenated anion $(M-H)^-$ at energies of around 1.5 eV [120, 123, 126, 127]. Early DEA studies ascribed this process to initial electron attachment into a π^* orbital of the (C=O) bond in the COOH group, which couples to the repulsive σ^* (O–H) orbital [118]. However, recent calculations questioned this DEA mechanism [126]; instead, it was suggested that direct electron capture into the purely repulsive short-lived σ^* (O–H) orbital, which is a very broad resonance of more than 5 eV width, could be responsible for the loss of the hydrogen [126].

In the condensed phase, analyzing LEE-stimulated desorption of anions from physisorbed thin films of glycine, alanine, cysteine, tryptophan, histidine, and proline [128, 129] indicated that H^- was the major desorption fragment, as CH_3^- , O^- , and OH^- were the fragments produced with lower signals in all named amino acids. Similar results were observed in ESD experiments from LEE-bombarded chemisorbed films, prepared by self-assembled monolayers (SAMs) of two different chains of Lys amide molecules [129]. For this model of a segment of a peptide backbone, the desorbed signals were dependent on the length of the amino acid sequence.

Amino acids are also suitable model molecules for investigating the interactions of biomolecules with metallic surfaces, particularly silver and gold. Of the 20 naturally occurring amino acids, only cysteine contains a thiol (-SH) group, which allows it to bind to the metal by forming a S-Metal bond [130, 131]. This characteristic makes cysteine an ideal model to investigate protein interactions with gold surfaces including those of gold nanoparticles [132, 133]. A detailed study on electron attachment to L-cysteine/Au(111) was recently reported by Alizadeh et al. [134, 135] who measured anion yields desorbed from chemisorbed (SAMs) and physisorbed thin films bombarded with sub-20 eV energy electrons. These ESD measurements

showed that LEEs are able to efficiently decompose this amino acid via DEA and dipolar dissociation (DD), when the molecule is chemisorbed via the SH group to a gold surface.

Regarding the protective effect of amino acids on DNA against LEEs, Solomun et al. [136] reported that the single-strand DNA-binding *E. coli* protein can effectively inhibit the formation of SSBs by 3-eV electrons in oligonucleotides. Ptasińska et al. [137] subsequently investigated by post-irradiation analysis with HPLC-UV, the molecular fragmentation induced by 1-eV electrons in films comprising the GCAT tetramer and one of the two amino acids, glycine and arginine. At low ratios (R) of amino acid to GCAT (i.e., $R < 1$), particularly for glycine, the total oligonucleotide fragmentation yield unexpectedly increased. At higher ratios ($1 \leq R \leq 4$), protection of DNA from damage by electrons was observed for both glycine and arginine. Therefore, the amino acid probably reduced electron capture by GCAT and/or the lifetime of the TMA that initiates DEA process. A similar conclusion regarding the stability of the amino acid side chain–nucleobase complexes can be deduced from the theoretical studies of Wang et al. [138]. Wang and coworkers performed calculations at the B3LYP/6-311G(d,p)-level anionic hydrogen-bonded complexes formed between the amino acid side chains and the nucleobase guanine.

Furthermore, by studying via first-principles molecular dynamics simulations a model system composed of thymine and glycine, Kohanoff et al. [139] recently investigated the protection of DNA by amino acids against the effects of LEEs. They considered thymine–glycine dimers and a condensed-phase model consisting of one thymine molecule solvated in amorphous glycine. These results indicated that at room temperature, the amino acid chemically and physically performs the role of a protective agent for the nucleobase. In a chemical mechanism, the excess electron is first captured by the thymine; then, a proton is transferred in a barrierless way from a neighboring hydrogen-bonded glycine. Reducing the net partial charge on the thymine molecule stabilizes the excess electron. In the physical mechanism, glycine molecule acts as an electron scavenger to capture the excess electron directly, which prevents the electron to be localized in DNA. Protecting the nucleobase via the latter mechanism requires a predisposition for proton transfer to the oxygen in the carboxylic acid group of one of the involved amino acids. Consequently, raising the free-energy barrier associated with strand breaks, prompted by these mechanisms, can halt further reactions of the excess electron within the strand of DNA, for instance, transferring the electron to the backbone which leads to induce a strand break in DNA. Increasing the ratio of amino acid to nucleic acid will enhance the protecting role of amino acids, and accordingly will decrease the induction of DNA strand breaks by LEEs, as shown experimentally [137, 139].

7. LEEs interaction and induced damage under cellular conditions

The gas- and condensed-phase experiments with DNA and its constituents discussed previously were performed under ultrahigh vacuum (UHV) conditions to permit use of electron beams and mass spectrometry, and to better control the molecular environment. While such experiments provide information on the direct effects of LEEs, they do not reveal how LEEs

can indirectly damage DNA. Comparatively, due to the experimental difficulties related to the production and observation of LEEs in aqueous media, studies on the indirect damage of LEEs to DNA have not been greatly developed.

Ideally, to understand how the fundamental mechanisms in LEE–DNA interactions are adapted in living cells, the experimental studies should be extended to the more complex dynamic molecular environment of the cell, or more realistic ones, for the DNA molecule that contains essentially water, oxygen, histones, and DNA-binding proteins [99]. For instance, in the work of Ptasíńska and Sanche [140], the ESD yields of different anions desorbed by 3–20 eV electron impact on GCAT films were measured under an aqueous condition, corresponding to 5.25 molecules of water per nucleotide. Their experiments demonstrated that adding water to dry DNA results in the binding of the molecule to the phosphate group at the negatively charged oxygen [141], and then formation of a complex of tetramer and a water molecule ($\text{DNA}\cdot\text{H}_2\text{O}$). This complex permits the formation of a new type of dissociative core-excited TMA located on the phosphate group, which decays by O^- desorption under electron impact via a resonance at 11–12 eV and by OH^- desorption from breaking the P–O bond. H^- also desorbs by dissociation of a TMA of the complex which causes bond cleavage on the H_2O portion. Moreover, LEE-induced damage to DNA via DEA enhances by a factor of about 1.6 when an amount of water corresponding to 60% of the first hydration layer is added to vacuum-dried DNA. Although the magnitude of this enhancement is considerable, it is still much smaller than the modification in yields of products produced by the first hydration layer surrounding the DNA during the radiochemical events that follow the deposition of the energy of LEE in irradiated cells. Theoretical and experimental studies were concurrently carried out on the diffraction of 5–30 eV electrons in hydrated B-DNA 5'-CCGGCGCCGG-3' and A-DNA 5'-CGCGAATTCGCG-3' sequences by Orlando et al. [142]. They postulated that compound $\text{H}_2\text{O}\cdot\text{DNA}$ states may contribute to the modification of strand breaks yield functions [142, 143]. Furthermore, Orlando et al. noted that lowering of the threshold energy for DSBs below 5 eV may be correlated with the presence of these compound states. In this case, an initial “core-excited” resonance would autoionize, yielding electronically excited water-derived states and a low-energy electron. The electronically excited state dissociates forming reactive O, OH, and H, which can lead to sugar–phosphate bond breakage. The slow electron could moreover scatter inelastically within a limited mean free path and excite a “shape” resonance of a base on the opposite strand. The combination of these two energy-loss channels could lead to a DSB. This type of DSB requires the presence of water and is difficult to be repaired due to the close proximity of damage sites.

Recent work using graphene-coated gold thin films also signaled the significance of the existence of water molecules in DNA damage mediated by “shape” resonances [144]. This is likely due to the influence of water on lowering the barrier for charge transfer from the base to the sugar–phosphate bond. In addition, the binding interaction of DNA with graphene allows direct coupling to the phosphates as well as more direct scattering with the guanine and adenine bases. Electrons that have not been captured by DNA bases can be captured by graphene and immediately transferred over 200 nm within < 0.36 ps. The environmental or graphene substrate interactions are critical, and at least two mechanisms occur simultaneously

during DNA damage on monolayer graphene: direct base capture and ballistic transfer from the graphene.

An alternative approach to simulate cellular conditions has been recently developed by Alizadeh et al. [145] to investigate LEE-induced DNA damage under atmospheric conditions and at various levels of humidity and oxygen. Thin films of plasmid DNA deposited on tantalum and glass substrates were exposed to Al K_{α} X-rays of 1.5 keV. The general features of the photo-ejected SE from the metallic surfaces exposed by primary X-ray photons are well understood; in particular, more than 96% of SEs emitted from tantalum lie below 30 eV and the energy distribution peaks around 1.4 eV, with an average energy of 5.85 eV [145]. Whereas the damages induced in DNA deposited on glass are due to soft X-rays, those arising from DNA deposited on tantalum result from the interaction of X-rays + LEEs. The difference in the damage yields measured in the samples deposited on two different substrates is ascribed to the interaction of LEEs with the DNA and its nearby atmosphere.

Alizadeh and Sanche [146] employed this technique to examine how the presence of several cellular components (such as, O_2 , H_2O and O_2/H_2O) modulates the LEE-induced damage to DNA molecules. They observed that for hydrated DNA films in an oxygenated environment, the additional LEE-induced damage that results from the combination of water and oxygen exhibits a super-additive effect, which produces a yield of DSB almost seven times higher than that obtained by X-ray photons. More recently, they reported the formation of four radiation-induced products from thymidine by soft X-rays and LEEs, specifically base release, and base modification including 5-HMdUrd, 5-FordUrd, and 5,6-DHT [147]. Of the products analyzed, thymine release was the dominant channel arising from N-glycosidic bond cleavage involving π^* low-lying TMA. A LEE-mediated mechanism was proposed to explain observation of 5-HMdUrd and 5-FordUrd products, which involve loss of hydride ($-H^-$) from the methyl group site via DEA. G -values derived from the yield functions indicate that formation of free thymine, 5-HMdUrd, and 5-FordUrd are promoted by an oxygen environment rather than a nitrogenous atmosphere, since the numbers and reactivity of radicals and ions are formed via interactions of radiation with O_2 , and are considerably larger than under N_2 . Moreover, O_2 can additionally react with C-centered radicals, thereby “fixing” or rendering the damage permanent. In contrast, no 5,6-DHT was detected when samples were irradiated under an O_2 atmosphere, indicating that O_2 molecules react with an intermediate radical compound, thereby inhibiting the pathway for 5,6-DHT formation [147].

Recently, novel decay mechanisms for electronic excitations and correlated electron interactions have become subjects of intense study. Just over a decade ago, Cederbaum et al. [148–150] proposed an ultrafast relaxation process in inner valence levels, which occurs in molecular systems with weakly bound forces, such as van der Waals forces or hydrogen bonding. This mechanism referred to as intermolecular Coulomb decay (ICD) is possible mainly due to the couplings and interactions induced by the local environment. Unlike most ionization processes, ICD results in the ejection of an electron from the neighbor of an initially ionized atom, molecule, or cluster [151]. The energy of the ICD electron is low, typically less than 10 eV. ICD is expected to be a universal phenomenon in weakly bound aggregates that contain light atoms and may represent a hitherto unappreciated source of LEEs. Though most ICD measurements

have concentrated on rare gas clusters, new sophisticated experimental approaches have detected ICD in large water clusters [152] or at condensed-phase interfaces containing water dimers and clusters [151].

Random damage to cellular biomolecules such as DNA is associated with the onset of cancer, whereas the controlled targeted local release and interactions of LEEs can be used as effective therapeutic cancer treatment agents. Since ICD is a source for the ejection of slow electrons, it has been proposed that ICD could play a role in the induction of SSB and DSB in DNA [153]. Estimation by Grieves and Orlando [152] indicated that ICD may represent up to 50% of the SSB probability for energy depositions >20 eV and ionization events directly at the DNA–water interface. Since the formation of DSBs requires excitation energies >5 eV, the impact on DSBs is expected to be much lower. If ICD contributes significantly to DNA damage, this could be exploited during X-ray treatment of cancer. **Figure 4** schematically shows that how utilizing of X-ray interactions with gold nanoclusters within living cells, which subsequently results in releasing both Auger and ICD electrons, has been suggested as a potential strategy for targeted cancer treatment [148].

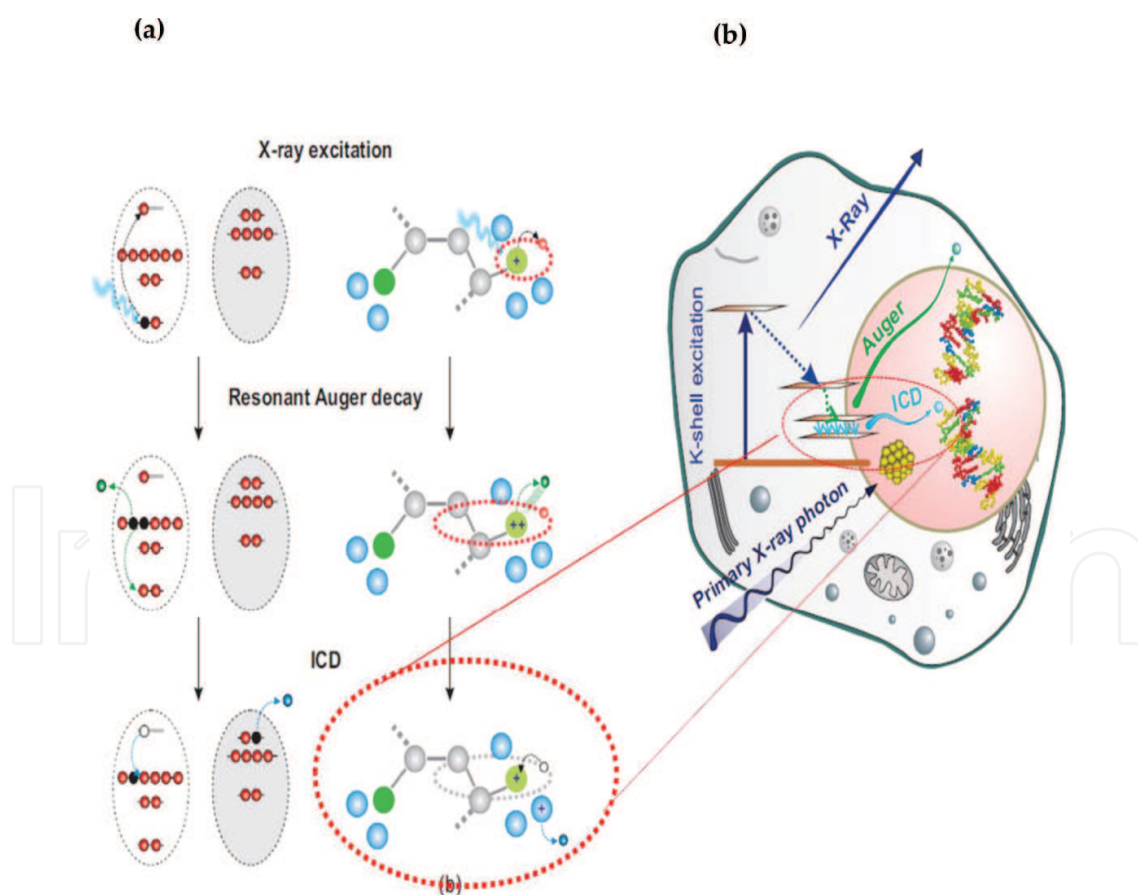


Figure 4. (a) Resonant Auger decay process following X-ray excitation. A second process known as interatomic or intermolecular Coulomb decay (ICD) can also occur, leading to the ejection of slow electrons and adjacent holes. (b) Possible exploitation of Au nanoparticles and ICD in the controlled radiation damage of cells [148].

After such extensive studies on LEE-induced damage under “near”-cellular conditions, it was only very recently that the lethal effects of LEEs in cells have been demonstrated by Sahbani et al. [154], who investigated the biological functionality of DNA, via a simple model system comprising *E. coli* bacteria and plasmid DNA bombarded by LEEs. In these experiments, highly ordered DNA films were arranged on pyrolytic graphite surface by molecular self-assembly technique using 1,3-diaminopropane ions to bind together the plasmid DNAs [155]. This assembly technique mimics somewhat the action of amino groups of the lysine and arginine amino acids within the histone proteins. These authors measured the transformation efficiency

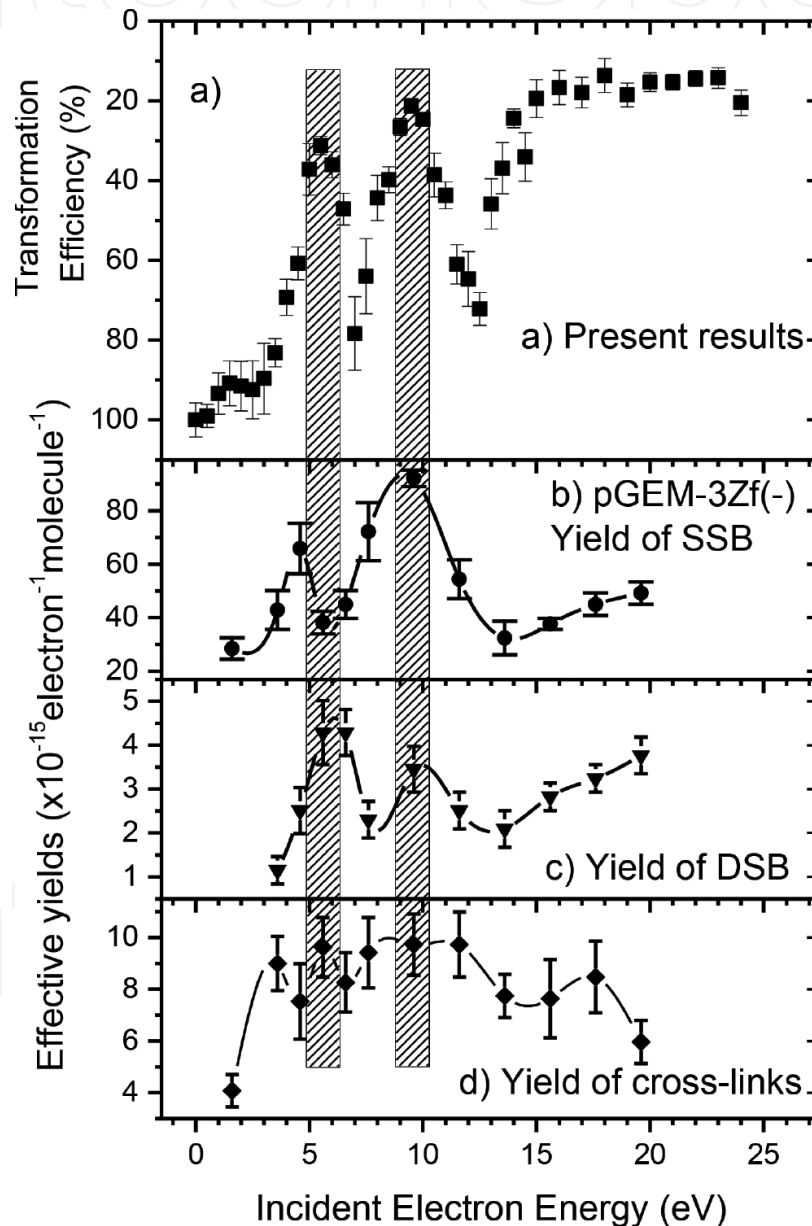


Figure 5. (a) Variation of transformation efficiency of *E. coli* by pGEM 3Zf(-) plasmids irradiated by 0.5–18 eV electrons at a fluence of 27×10^{13} electrons/cm². The vertical axis is inverted. Effective yield functions for (b) single-strand breaks (SSBs), (c) double-strand breaks (DSBs), and (d) DNA cross-links [183].

of *E. coli* JM109 bacteria (essentially the number of bacterial colonies grown in an antibiotic environment) after insertion into the cells of [pGEM-3Zf (-)] plasmid, which when undamaged, can confer resistance to the antibiotic ampicillin. Before transformation, the plasmids were irradiated with electrons of specific energies in the energy range 0.5–18 eV [156]. Cells receiving severely damaged plasmids will not grow, and the transformation efficiency will be reduced. The loss of transformation efficiency plotted as a function of electron energy is shown in **Figure 5**. It reveals maxima at 5.5 and 9.5 eV, coincident with the maxima observed in the yields of DNA DSBs, which were attributed to the formation of core-excited TMAs. These results indicated that the effects of TMAs are observable in the electron-energy dependence of biological processes with negative consequences for cell viability. The result provides further evidence that LEEs play important roles in cell mutagenesis and death during radiotherapeutic cancer treatment [156].

8. Role of LEEs in radiosensitization and radiation therapy

A major impetus for achieving a better understanding of the action of ionizing radiation in biological systems relates to applications in radioprotection and radiotherapy. Since LEEs play a major role in transferring the energy of the initial high-energy particle or photon to initiate all subsequent chemistry in irradiated media, understanding their interaction with biomolecules is now being recognized as a crucial and essential step toward such applications. As seen from Section 4, in the last decades, our expanding knowledge of LEE–DNA interactions has been applied to experiments involving known radiosensitizers. Both at the theoretical and experimental levels, this work served to suggest new compounds having radiation-damage enhancing properties and to explain the details of their response to high-energy radiation either alone or when bound to DNA (i.e., the main target for cell killing in radiotherapy).

8.1. Transient anions in halogen compounds

Bromouracil, which can replace thymine in DNA during cell replication, and bromouridine were the first radiosensitizing candidates to be investigated theoretically and experimentally with LEEs. The studies [157–167] confirmed the prediction of Zimbrick and coworkers [168] that the radiosensitizing properties of these compounds arose from DEA of solvated electrons, and further showed that DEA of higher energy (0–7eV) electrons was also involved in radiosensitization. Platinum bromide, aromatic compounds containing nitro group and other halogenated thymidine derivatives were found to play similar roles [58, 70, 71, 163–165, 169, 170]. Following early investigations with solvated electrons [168], a relatively large number of experiments have been performed both in the gas (see Section 4.4) and condensed phases [160, 161, 165] to study electron scattering from—and attachment to—halogenated pyrimidines. Several experiments were performed using SAMs of BrdU-containing oligonucleotides [157, 158, 171]. These included the detection of the electron-stimulated desorption of ion and neutral species and HPLC analysis of damaged films, as well as electronic and vibrational electron-energy loss spectra for gaseous bromouracil [159]. These studies revealed that the radiosensi-

tization properties of halogen compounds are more complicated than previously anticipated [168]. Within the 0–7 eV energy range, resonant electron scattering mechanisms with halouracils lead to more complex molecular fragmentation than that occurs with thymine, which produces a different range of anionic and neutral radical fragments. When formed within DNA, such fragments could react with local subunits, and thus lead to lethal clustered damage, further to that already occurring in unsensitized DNA. The most striking evidence of a huge enhancement of LEE damage obtained upon Br substitution in thymine is seen in the early results of Klyachko et al. [160], who found that, in the presence of water, DEA to bromouracil could be enhanced by orders of magnitude compared to the dry compound. Differences between wet and dry TMA states of halogenated pyrimidines have recently been investigated by Cheng et al. [172]. They applied Koopman's theorem in the framework of long-range corrected density functional theory for calculation of the TMA states and self-consistent reaction field methods in a polarized continuum to account for the solvent. Their results indicate that the TMAs of these molecules are more stable in water, but to differing degrees.

The radiosensitization properties of halouracils depend not only on hydrated electrons, but also on LEEs and on DEA. However, the high propensity of LEEs of very low energies (i.e., <1 eV) to fragment bromouracil and deoxybromouridine (BrUdR) may, according to the theory, exist only in single-stranded DNA [165]. This important prediction was confirmed by Cecchini et al. [173] for the case of solvated electrons and was commented upon by Sevilla [174]. Solutions of single- and double-stranded oligonucleotides, and of double-stranded oligos containing mismatched bubble regions, were irradiated with γ -rays, and the concentrations of various reactive species produced, including solvated electrons, were controlled with scavengers. When in the absence of oxygen, OH radicals were scavenged, BrUdR was shown to sensitize single-stranded DNA, but could not sensitize complementary double-stranded DNA. However, when BrUdR was incorporated in one strand within a mismatch bubble, the nonbase-paired nucleotides adjacent to the BrUdR, as well as several unpaired sites on the opposite unsubstituted strand, were highly sensitive to γ -irradiation. Since LEEs and solvated electrons fragment BrUdR by the same DEA mechanism [162–165, 168], these results imply that the strong sensitizing action of BrUdR to electron-induced damage is limited to single-stranded DNA, which can be found in transcription bubbles, replication forks, DNA bulges, and the loop region of telomeres. These results are clinically relevant since they suggest that BrUdR sensitization should be greatest for rapidly proliferating cells [173, 174]. When injected into a patient being treated for cancer, BrUdR quickly replaces a portion of the thymidine in the DNA of the fast-growing malignant cells, but radiosensitization occurs only when DNA is in a single-stranded configuration (e.g., at the replication forks during irradiation). From this conclusion, it appears advantageous to administer to patients receiving BrUdR, another approved drug, such as hydroxyurea, to increase the duration of the S-phase of cancer cells (i.e., the replication cycle). This addition would increase the probability that SEs would interact with bromouracil while bound to DNA in its single-strand form. Such a modality provides an example of how our understanding the mechanisms of LEE-induced damage can help to improve radiotherapy [174].

8.2. Transient anions in DNA bound to platinum chemotherapeutic agents

Considering that it can often take years, if not decades, before potential new radiosensitizers arrive in the clinic, Zheng et al. [175] hypothesized that present clinical protocols involving high-energy radiation and platinum (Pt) chemotherapeutic agents could be improved by considering the fundamental principles of energy disposition, including the results of LEE experiments. Their initial goal was to explain the superadditive effect occurring in tumor treatments, when cisplatin and radiation were administered in concomitance [176, 177]. Zheng et al. [175] found that, with cisplatin bound to DNA as in the cancer cells, damage to the molecule increases by factors varying from 1.3 for high-energy electrons to 4.4 at 10 eV. Considering the much higher enhancement factor (EFs) at 10 eV, the increase in bond dissociation was interpreted as being triggered by an increase in DNA damage induced by LEEs.

In their experiments, Zheng et al. [175] deposited lyophilized films of pure plasmid and plasmid–cisplatin complexes on a clean tantalum foil. The films were bombarded under UHV with electrons of 1–60 keV. Under these conditions, 90% of the plasmid–cisplatin complexes consisted of a cisplatin molecule chemically bound to DNA, preferentially at the N7 atom of two guanines producing an interstrand adduct. The films had the necessary thickness to absorb most of the energy of the electrons. The different forms of DNA corresponding to SSBs and DSBs were separated by gel electrophoresis, and the percentage of each form quantified by fluorescence. Exposure response curves were obtained for several incident electron energies for cisplatin bound or not to plasmid DNA. **Table 1** gives the results for exposure to 1, 10, 100, and 60,000 eV electrons of films of pure DNA and cisplatin/plasmid complexes with a ratio (*R*) of 2:1 and 8:1. For both *R* values, cisplatin binding to DNA increases the production of SSBs and DSBs, but in quite different proportions depending on electron energy. Considering that it takes about 5 eV to produce a DSB with electrons [90], the most striking result of **Table 1** is clearly the production of DSBs by 1 eV electrons. Later, Rezaee et al. [178] demonstrated that even 0.5 eV electrons could induce DSBs in DNA containing Pt adducts in similar proportions and more efficiently than other types of radiation, including X-rays and high-energy electrons. The formation of DSBs by 0.5 eV electrons resulted from a single-hit process. Gamma radiolysis experiments with plasmid DNA dissolved in water, further demonstrated that even solvated electrons could react with cisplatin–DNA complexes to induce DSBs [179]. The results of Zheng et al. [175] at higher energy were later confirmed by those of Rezaee et al. [180], who showed that increased damage via the formation of TMA could explain, at least partially, the concomitance effect in chemoradiation therapy for cisplatin, as well as for the other platinated chemotherapeutic drugs such as oxaliplatin and carboplatin.

This type of radiosensitization was investigated in more detail by irradiating with a γ source the oligonucleotide TTTTGTGTTT with or without cisplatin bound to the guanines [181]. Using scavengers and by eliminating oxygen, the oligonucleotide was shown to react with hydrated electrons. Prior to irradiation, the structure of the initial cisplatin adduct was identified by mass spectrometry as G-cisplatin-G. Radiation damage to DNA bases was quantified by HPLC, after enzymatic digestion of the TTTTGTGTTT–cisplatin complex to deoxyribonucleosides. Platinum adducts were following digestion and separation by HPLC, quantified by mass spectrometry. The results demonstrated that hydrated electrons induce

damage to thymines as well as detachment of the cisplatin moiety from both guanines in the oligonucleotide. The amount of free cisplatin (i.e., the cleavage of two Pt–G bonds) was found to be much larger than that of the products resulting from the cleavage of a single bond [181,182].

Form of damage	SSB				DSB			
	1	10	100	60,000	1	10	100	60,000
Energy (eV)								
Thickness	5 ML				2900 nm			
DNA	27 ± 3	33 ± 3	57 ± 5.5	1.2 ± 0.1	ND	10 ± 1	13 ± 2	0.4 ± 0.2
Cisplatin:DNA = 2:1	38 ± 3	120 ± 11	150 ± 15	2.4 ± 0.3	5 ± 1	17 ± 1	36 ± 4	0.5 ± 0.2
Cisplatin:DNA = 8:1	52 ± 5	143 ± 14	199 ± 18	3.0 ± 0.4	5 ± 2	29 ± 2	44 ± 4	0.7 ± 0.1

ND, Not detected.

The errors represent the deviation of three identical measurements.

Table 1. Yields (in 10^{-15} electron $^{-1}$ molecule $^{-1}$) for the formation of SSB and DSB induced by 1, 10, and 100 eV electron impact on 5 ML DNA films and 60 keV electron impact on 2900 nm DNA films deposited on a tantalum substrate.

These results suggest two major pathways by which hydrated electrons interact destructively with TTTTGTGTTT–cisplatin [181, 182]. First, the hydrated electron is captured initially on a thymine base and is transferred to the guanine site by base to base electron hopping, where DEA detaches the cisplatin moiety from the oligonucleotide. Alternatively, the hydrated electron interacts directly with the platinum–guanine adduct, and cisplatin is detached via DEA. These hypotheses were consistent with those proposed by Rezaee et al. [178] for LEE-induced damage to plasmid DNA. Additionally, Rezaee et al. suggested that in the double-stranded configuration, the cisplatin molecule weakens many of the DNA chemical bonds and changes the topology of the molecule; these modifications render DNA much more sensitive to damage over large distances [180]. Of course, under high-energy irradiation conditions, the increase in ionization cross section, due to the presence of the Pt atom, also increases the quantity of LEEs near cisplatin and therefore may indirectly contribute to the increase in damage.

More recently, the energy dependence of conformational damage induced to pure plasmid DNA [183] and cisplatin–plasmid DNA complexes [184] was investigated in the range 2–20 eV. In addition to the strong resonances (i.e., TMAs) in pure DNA around 5 and 10 eV, further TMA specific to cisplatin-modified DNA were observed in the yield function of SSBs at 13.6 and 17.6 eV. Moreover, the presence of cisplatin lowered the threshold energy for the formation of DSBs to 1.6 eV, considerably below that observed with electrons in pure DNA films. In all cases, the measured yields were larger than those measured with nonmodified DNA. To reconcile all existing results starting from those obtained with hydrated electrons to those generated up to 20 eV, Bao et al. [184] suggested a single mechanism that could apply to shape and core-excited resonances, depending or not if electronic excitation of the Pt or guanines was involved in TMA formation. This mechanism, previously proposed for shape resonances by

Rezaee et al. [178], can be explained with reference to **Figure 6**. When the TMA is formed on the Pt adduct, the extra electron is delocalized and occupies simultaneously, with identical wave functions, the two bonds linking the Pt atom to guanine bases on opposite strands. Occupancy of the dissociative σ^* orbitals induces equal repulsive impulses on the two bonds between platinum and guanines (Pt–G), due to the symmetrical delocalization of the excess electron. If the extra electron autodetaches when the gained kinetic energy is larger than the energy barrier to dissociate the Pt–G bonds, both bonds can be simultaneously broken. The extra energy for dissociation is supplied to the complex by autodetachment from the σ^* bond, leaving the additional electron stabilized at the bottom of the potential well of the Pt. The simultaneous cleavage of two Pt–G bonds and formation of two guanine radicals are followed

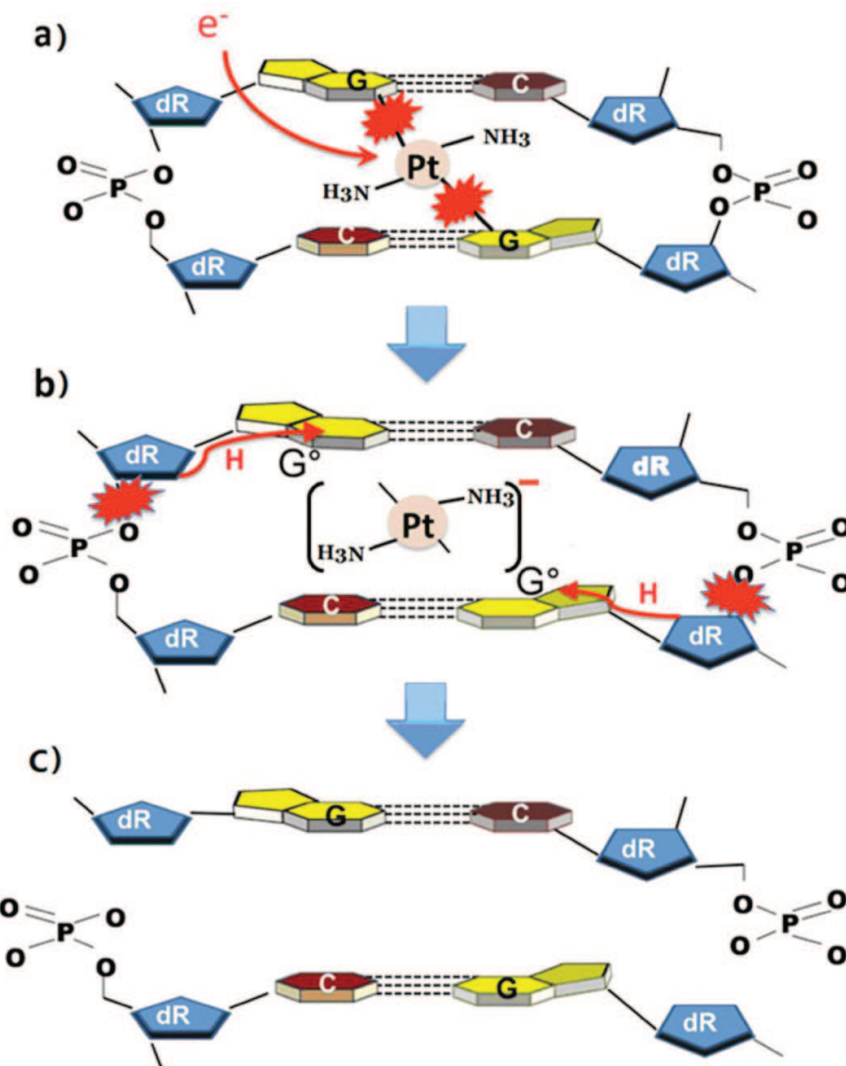


Figure 6. Possible mechanism for the formation of a DSB by a single electron, when cisplatin links two guanine (G) bases on opposite strands. (a) Electron capture into two identical dissociative orbitals between Pt and two Gs. (b) The transient anion thus formed dissociates, leaving the electron on the (NH₃)₂Pt moiety and causing simultaneous cleavage of the two symmetrical Pt–G bonds. The resulting two guanine radicals (G[•]) abstract hydrogen from the backbones, causing cleavage of phosphodiester bonds on opposite strands. (c) Resulting DSB [178].

by hydrogen abstraction from the backbone. This abstraction cleaves the phosphodiester bonds in opposite strands, forming a DSB. Considering the results obtained with carboplatin and oxaliplatin [180], which are similar to those obtained with cisplatin, the mechanism depicted in the diagram of **Figure 6** is likely to apply also to these chemotherapeutic drugs. Since these latter behave as cisplatin and bind similarly to DNA, we can replace cisplatin by carboplatin in **Figure 6**; to represent oxaliplatin in the figure, NH_3 has to be replaced by $\text{C}_6\text{H}_{10}(\text{NH}_2)_2$.

The LEE enhancement mechanism of damage in DNA–Pt drug complexes acts on a femtosecond timescale, which quite unlike other biological mechanisms of radiosensitization, act over macroscopic times that can range from hours to days. These considerations imply that the mechanism (e.g., physicochemical vs biological) of radiosensitization by Pt agents in concomitant chemoradiation therapy may be sensitive to the timing between the injection of the drug to the patient and the irradiation. Thus, if TMA formation in DNA plays a major role in radiosensitization by Pt drugs, maximal cancer cell killing should be achieved, if these cells are irradiated when the maximum amount of Pt is bound to their nuclear DNA.

Led by this hypothesis, Tippayamontri et al. [185, 186] determined the optimal conditions for concomitant chemoradiation treatment of colorectal cancer with cisplatin, oxaliplatin, and their liposomal formulations Lipoplatin and Lipoxal [187, 188]. Using an animal model of human colorectal cancer, they determined the time window for maximum radiosensitization and synergy with irradiation, by studying the pharmacokinetics and time-dependent intracellular distribution of the Pt drugs. This, in turn, is determined by the reaction kinetics of the drug with DNA and the DNA repair kinetics.

In nude mice bearing HCT116 colorectal carcinoma, treated with the Pt drugs, they measured by inductively coupled plasma mass spectrometry, the platinum accumulation in blood, serum, different normal tissues, tumor, and different tumor cell compartments, including the amount of Pt bound to nuclear DNA [185, 186] **Figure 7a** indicates the positions of binding of cisplatin to DNA. Examples of the amount of cisplatin and Lipoplatin binding to the DNA of HCT116 colorectal cancer cells in mice are shown in **Figure 7b** as a function of time after injection of the drug. Radiation treatment (15 Gy) was given 4, 24, and 48 h after drug administration. The resulting tumor growth delay was reported and correlated with apoptosis analyses. Optimal survival of the mice and highest apoptosis were observed when radiation was given at 4 or 48 h after drug injection. These times corresponded to the times of maximal platinum binding to tumor DNA, as shown in **Figure 7b** for cisplatin and Lipoplatin. When tumor irradiation was performed at 48 h, the ratio of tumor growth delay for the group having the combined treatment compared to delay for the group treated with chemotherapy alone varied from 4.09 to 13.00, depending on the drug. The most efficient combination treatment was observed when the amount of Pt drug binding to DNA was highest, as predicted from fundamental considerations [178–182]. Such results testify our fundamental understanding of the mechanisms of platinum-induced radiosensitization and should have significant impact on the design of more efficient treatment protocols.

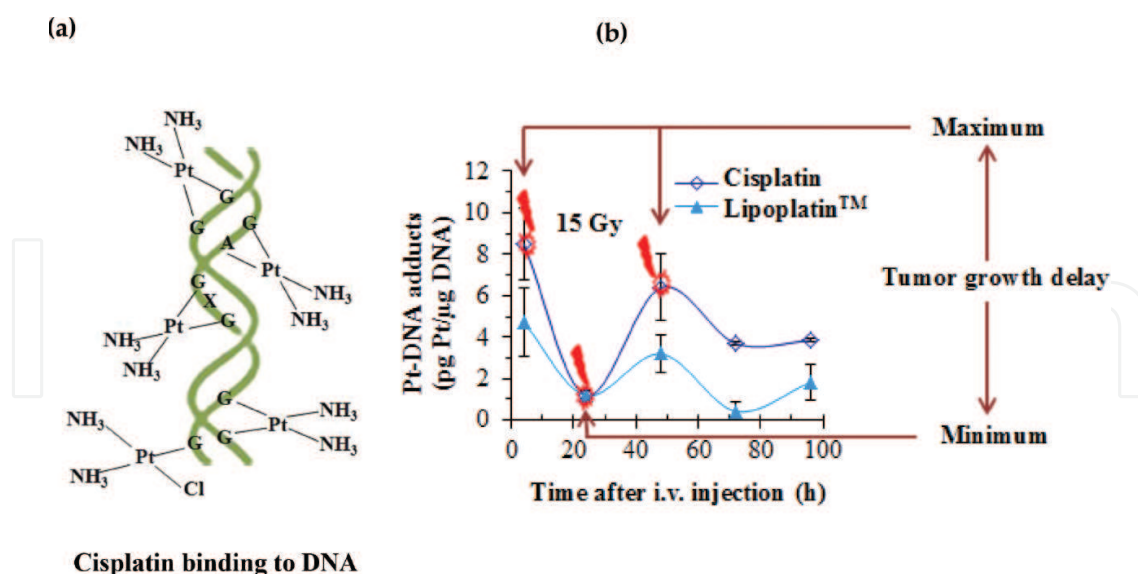


Figure 7. (a) Diverse sites of intrastrand and interstrand binding of cisplatin to cellular DNA. (b) Concentration of Pt-DNA adducts in the nucleus of human colorectal cancer cells of mice bearing HCT116 xenografts, as a function of time after administration of cisplatin and Lipoplatin™. The mice were irradiated at 4, 24, and 48 h after injection of the chemotherapeutic agents.

8.3. Interaction of LEEs with DNA bound to gold nanoparticles

So far in this section, we have shown that cancer cells can be made more sensitive to high-energy radiation by chemically modifying their nuclear DNA with small molecules. These latter provide at least some of their radiosensitizing action, by increasing the interaction of LEEs with DNA, the products of DEA, and the resulting induced damage. Another approach consists of simply increasing the numbers of LEEs near the DNA of cancer cells. The best examples of this type of radiosensitization have been provided by the numerous fundamental, *in vitro*, and *in vivo* investigations of enhanced radiation absorption by gold nanoparticles (GNPs).

Both *in vitro* and *in vivo* experiments [189–204] have shown radiation enhancement effects due to the presence of GNPs. Several models have been developed to account for dose enhancement in cells by considering the increase in radiation energy deposition [205–211], due to additional energy absorption by the GNPs, as a function of their size. As expected, the energy of electrons emanating from the GNPs is inversely proportional to their diameter. Many models [206–211] take into account localized effects of Auger-electron cascades. They consider the huge enhancement of energy deposited in the vicinity of GNPs, as arising from the considerable increase in photoelectric absorption cross section of gold in comparison to that of tissue [200, 208, 210, 211]. The increase in this cross section produces an additional local generation of photoelectrons, Auger electrons, and characteristic X-rays [208, 212]. The major portion of the energy absorbed by the GNPs is converted into electrons, most of which escapes the GNPs with low energy (0–30 eV) [213–215].

The indirect effect of emitted electrons was investigated in water solutions containing GNPs, where the nanoparticle-induced OH concentration from radiolysis was measured. Relevant literature and details can be found in the paper of Sicard-Roselli et al. [189], who also proposed a new mechanism for hydroxyl radical production in irradiated GNP solutions.

The direct effect of high-energy radiation on DNA, resulting from the presence of GNPs, was first investigated by Zheng and coworkers [35, 214–218]. Relatively thick (~0.3 and 2.9 μm) films of plasmid DNA with or without electrostatically bound GNPs were bombarded with 60 keV electrons. The probabilities of formation of SSBs and DSBs from the exposure of 1:1 and 2:1 GNP–plasmid mixtures to fast electrons increased by a factor of about 2.5, compared to DNA alone. It was suggested that the additional damage in the presence of GNPs was generated by LEEs escaping the nanoparticles. This hypothesis was later verified experimentally by the work of Xiao et al. [214]. These authors investigated the radiosensitization efficiency in terms of DNA damage as a function of the length of a ligand bound at one end to the surface of the GNP and at the other to DNA. They used the same DNA film preparation as in the experiments of Zheng et al. [215] and measured the ratio of induced damage with GNPs to that without GNPs (i.e., the enhancement factor, EF) for different lengths of the ligand. As indicated in **Figure 8** from their work, the corresponding EFs induced by 60 keV electrons on plasmid DNA bound to GNPs of various coatings range from 2.3 to 1.6 and 1.2, depending on the length of ligand separating the gold surface from the plasmid. This length ranged from 0 to 2.5 and 4 nm, respectively. The attenuation by the coating of short-range LEEs emitted from the GNPs could explain the decrease in radiosensitization with increasing length of the ligand [214]. Since the attenuation range of LEEs is shorter than about 10 nm, it is obvious that the emission of LEEs from the GNPs and LEE–interaction with DNA plays a major role in the mechanism of GNP radiosensitization.

Later, similar DNA–GNP films were bombarded with electrons of energies below the ionization potential of DNA. In this case, essentially no secondary LEEs were emitted from the DNA and the gold surface, so that Yao et al. [218] could investigate the purely chemical radiosensitization induced by GNPs. They showed that even without the emission of photoelectrons, direct electrostatic binding of an average of 0.2–2 GNPs to DNA could increase sensitization to LEEs by factors varying from 1.5 to 4.

Since GNPs increase the local density of LEEs and cisplatin enhances LEE interactions with DNA and damage to the molecule, it seemed likely that binding GNPs to a cisplatin–DNA complex would further boost radiosensitization and DNA damage induced by cisplatin [216]. This hypothesis was verified by irradiating with 60 keV electrons, GNPs electrostatically bound to a cisplatin–DNA complex [216]. Dry films of bare plasmid DNA and DNA–cisplatin, DNA–GNP, and DNA–cisplatin–GNP complexes were irradiated [216]. The yields of SSBs and DSBs were measured as described in the protocol established by Zheng et al. [215]. When the ratio of GNP to DNA was 1:1 and that for cisplatin to DNA was 2:1, the EFs for SSBs were between 2 and 2.5. With a cisplatin to GNP to plasmid ratio of 2:1:1, the EF increased to 3. This small increase could only be additive and unrelated to the interaction of additional LEEs with cisplatin. For DSB formation, however, the binding of both GNPs and cisplatin to a DNA molecule produced an impressive increase in the EF, that is, DSBs were increased by a factor

of 7.5 with respect to pure DNA. It appeared quite obvious that the additional DSBs in the cisplatin–DNA–GNP complex arose from the generation of additional secondary electrons from the GNPs. The synergy between GNPs and cisplatin could arise from a number of basic phenomena, including the possibility of two or multiple event processes triggered by the interaction of a single 60 keV electron with a GNP. Within 10 nm of its location, a single gold atom increases the density of LEEs by a large factor [207, 212], and hence, a GNP that contains thousands of gold atoms is expected to generate a dramatic increase in this density [213]. Combined with the fact that cisplatin considerably lowers the energy threshold for DSB formation, a single or multiple LEE interactions on opposite strands within a distance of 10 base pairs could increase considerably the number of DSBs formed in GNP–cisplatin–DNA complexes.

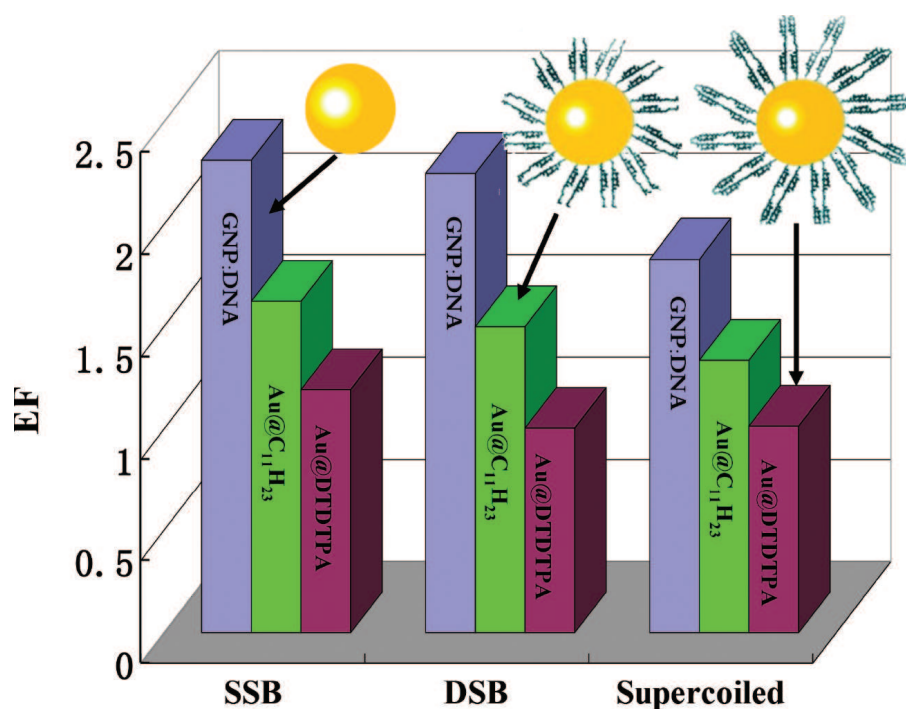


Figure 8. Enhancement factors (EFs) for the formation of SSB, DSB, and loss of supercoiled DNA induced by 60 keV electrons, obtained with GNP–DNA complexes of ratio 1:1. The groups of three histograms represent the respective damages. In each group, the EF corresponds to the damage when the GNP alone is bound to DNA or when the GNP has been coated with ligands 2.5 and 4 nm in lengths corresponding to GNP@C₁₁H₂₃ or GNP@DTDTPA (i.e., dithiolated diethylenetriaminepentaacetic acid), respectively in the figure.

As shown by Zheng et al., only one GNP per DNA molecule is on average necessary to increase DNA damage considerably [216]. Thus, as long as the nanoparticles reach the DNA of cancer cells, the amount to be administered to patients to obtain significant radiosensitization should be at most the same as that of the Pt-drugs routinely administered in chemotherapy [176, 177]. In recent *in vitro* experiments, GNPs were targeted to the DNA in the cell nucleus by linking peptides to the gold surface [197, 202]. Such vectored GNPs, targeting the DNA of cancer cells, should be applicable in the clinic and may accordingly offer a new approach to radiotherapy treatments. However, this type of radiotherapy is expected to be limited to

superficial tumors, owing to the requirement for that low-energy (<100 keV) X-rays be used to optimize LEE production and hence radiosensitization by the photoelectric effect. To treat deep tumors, a radioactive source may have to be encapsulated inside a gold nanoparticle (i.e., in a gold nanocage) [219]. Furthermore, if DNA specificity cannot be achieved in patients, successful treatment may still be possible by intratumor injection of GNPs, as recently shown by Shi et al. [220] and Bobyk et al. [204].

9. Summary and Conclusions

The experimental and theoretical results of LEE impact on single- and double-stranded DNA, its basic constituents, protein subunits, as well as radiosensitizers and chemotherapeutic agents alone or bound to DNA were reviewed. Experimental details of LEE interactions with these biomolecules were obtained in both the condensed and gas phases. The condensed-phase experiments were conducted in UHV and at atmospheric pressure under environments closer to those of the cell. From these studies, which provide a fundamental comprehension of the role of TMAs in irradiated biological systems, we can arrive with considerable certainty at the following conclusions on LEE-induced damage to biomolecules. In the low-energy range (i.e., below the threshold for dipolar dissociation (~15 eV)), bond rupture in biomolecules occurs essentially via the formation of TMAs that decay either via autoionization with the accompanied production of dissociative electronically excited states, or into the DEA channel. The induced damage depends on a large number of factors, including electron energy, the environment and topology of the molecule, and the electrostatic or chemical binding of small radiosensitizing molecules. Such factors inevitably modify the lifetime and decay channels of transient anions, which often increase the damage cross sections.

Since secondary electrons of low energy possess a large portion of the energy deposited by high-energy radiation, any modification of how their energy deposits at crucial cellular sites is expected to have a strong radioprotective or radiosensitizing action. With DNA being the main target in radiotherapy, parameters that affect LEE-induced DNA damage are necessarily of relevance to radiosensitivity, and the mechanisms involved must be well understood to control and modulate the biological effects of ionizing radiation.

Many of these mechanisms are now well established as seen from the experiments and theoretical treatments reviewed in this chapter. Moreover, it has been shown that applying fundamental principles of action of LEEs to radiosensitizers or chemotherapeutic agents can lead to new strategies on how to improve radiotherapy outcomes. In particular, the role of LEEs in radiation damage was related to enhancement of the destruction of cancer cells by Pt-drugs and gold nanoparticles. LEEs were found to play an important role in providing guidelines in chemoradiation cancer treatment, as well as in the development of more efficient clinical protocols. Such applications point out the need for multidisciplinary studies in this field, where LEE–biomolecule interactions have become an area of intensive investigation that encompasses many aspects of cancer therapy.

Acknowledgements

The authors gratefully express thanks for helpful comments of Dr. Andrew D. Bass and Dr. Darel J. Hunting. LS acknowledges the financial support from Canadian Institute of Health Research (CIHR, via MOP 81356 and 86676) and from Natural Sciences and Engineering Research Council of Canada (NSERC). S.P. acknowledges the financial support from the U.S. Department of Energy Office of Science, Office of Basic Energy Sciences under award number DE-FC02-04ER15533.

Abbreviations

A	adenine
AFM	atomic force microscopy
APPJ	atmospheric pressure plasma jet
C	cytosine
C	circular
CL	cross-link
CRT	chemoradiation therapy
DD	dipolar dissociation
DEA	dissociative electron attachment
DNA	deoxyribonucleic acid
DSB	double-strand break
EF	enhancement factor
ESD	electron-stimulated desorption
ESI	electrospray ionization
eV	electron volt
F-C	Franck-Condon
G	guanine
GNP	gold nanoparticle
HPLC	high-performance liquid chromatography
ICD	intermolecular Coulombic decay
keV	kilo electron volt
Kr	krypton
L	linear
LEE	low-energy electron
MALDI	matrix-assisted laser desorption ionization

MDSB	multiple double-strand break
MeV	mega electron volt
ML	monolayer
nm	nanometer
ps	picosecond
Pt	platinum
SAM	self-assembled monolayer
SC	supercoiled
SE	secondary electron
SERS	surface-enhanced Raman spectroscopy
SSB	single-strand break
T	thymine
TMA	transient molecular anion
U	uracil
UHV	ultrahigh vacuum
UV	ultraviolet
VFR	vibrational Feshbach resonance

Author details

Elahe Alizadeh^{1*}, Sylwia Ptasińska² and Léon Sanche³

*Address all correspondence to: ealizade@uoguelph.ca

1 Department of Chemistry and Biochemistry, University of Guelph, Guelph, ON, Canada

2 Radiation Laboratory and Department of Physics, University of Notre Dame, Notre Dame, IN, USA

3 Groupe en Sciences des Radiations, Département de Médecine Nucléaire et Radiobiologie, Faculté de médecine et des sciences de la santé, Université de Sherbrooke, Sherbrooke, QC, Canada

References

- [1] Lehnert S. Biomolecular Action of Ionizing Radiation. 1st ed. New York: Taylor and Francis; 2007. DOI: 10.1201/9781420011920

- [2] Baccarelli I, Bald I, Gianturco FA, Illenberger E, Kopyra J. Electron-induced damage of DNA and its components: experiments and theoretical models. *Phys. Rep.* 2011; 508: 1–44. DOI: 10.1016/j.physrep.2011.06.004
- [3] Denifl SP, Märk TD, Scheier P. The role of secondary electrons in radiation damage. In: Gomez-Tejedor GG, Fuss MC (eds). *Radiation Damage in Biomolecular Systems*. 1st ed. New York: Springer Science & Business Media; 2012. p. 45–58. DOI: 10.1007/978-94-007-2564-5. Ch 2.
- [4] Hall, EJ, Giaccia AJ. *Radiobiology for the Radiologist*. 6th ed. Philadelphia: Lippincott Williams and Wilkins; 2006. DOI: 10.1667/RR0771.1
- [5] Kufe DW, Pollock RE, Weichselbaum RR, Bast RC, Gansler TS, Holland JF, Frei E. *Holland-Frei Cancer Medicine*. 6th ed. Hamilton: BC Decker; 2003. ISBN-10: 1-55009-213-8
- [6] O'Driscoll M, Jeggo PA. The role of double-strand break repair: insights from human genetics. *Nat. Rev. Genet.* 2006; 7: 45–54. DOI: doi :10.1038/nrg1746
- [7] Alizadeh E, Orlando TM, Sanche L. Biomolecular damage induced by ionizing radiation: the direct and indirect effects of low-energy electrons on DNA. *Ann. Rev. Phys. Chem.* 2015; 66: 379–398. DOI: 10.1146/annurev-physchem-040513-103605
- [8] Sevilla MD, Bernhard WA. Mechanisms of direct radiation damage to DNA. In: Spothem-Maurizot M, Mostafavi M, Douki T, Belloni J (eds). *Radiation Chemistry: From Basics to Applications in Material and Life Sciences*. 1st ed. Les Ulis: EDP Sciences; 2008. p. 191–201. DOI:10.1002/cphc.201300915. ch13
- [9] Pimblott SM, La Verne JA. Production of low-energy electrons by ionizing radiation. *Radiat. Phys. Chem.* 2007; 76: 1244–1247. DOI: 10.1016/j.radphyschem.2007.02.012
- [10] Sanche L. Low-energy electron interaction with DNA: bond dissociation and formation of transient anions, radicals, and radical anions. In: Greenberg MM (ed). *Radical and Radical Ion Reactivity in Nucleic Acid Chemistry*. 1st ed. New Jersey: John Wiley and Sons; 2009. p. 239–293. DOI: 10.1002/9780470526279. ch9
- [11] Alizadeh E, Sanche L. Precursors of solvated electrons in radiobiological physics and chemistry. *Chem. Rev.* 2012; 112: 5578–5602. DOI: 10.1021/cr300063r
- [12] Sulzer P, Mauracher A, Denifl S, Zappa F, Ptasíńska S, Beikircher M, Bacher A, Wendt N, Aleem A, Rondino F, Matejcik S, Probst M, Märk TD, Scheier P. Identification of isomers of nitrotoluene via free electron attachment. *Anal. Chem.* 2007; 79: 6585–6591. DOI: 10.1021/ac070656b
- [13] Gu J, Xie Y, Schaefer HF. Electron attachment to hydrated oligonucleotide dimers: Guanylyl-3',5'-cytidine and cytidylyl-3',5'-guanosine. *Chem. Eur. J.* 2010; 16: 5089–5096. DOI: 10.1002/chem.200902977

- [14] Arumainayagam, CR, Lee HL, Nelson RB, Haines DR, Gunawardane RP. Low-energy electron-induced reactions in condensed matter. *Surf. Sci. Rep.* 2010; 65: 1–44. DOI: 10.1016/j.surfrep.2009.09.001
- [15] Schulz GJ. Resonances in electron impact on diatomic molecules. *Rev. Mod. Phys.* 1973; 45: 423–486. DOI: 10.1103/RevModPhys.45.423
- [16] Allan M. Study of the triplet-states and short-lived negative-ions by means of electron impact spectroscopy. *J. Electron. Spectrosc. Relat. Phenom.* 1989; 48: 219–351. DOI: 10.1016/0368-2048(89)80018-0
- [17] Sanche L. Primary interactions of low-energy electrons in condensed matter. In: Jay-Gerin J-P, Ferradini C (eds). *Excess Electrons in Dielectric Media*. 1st ed. Boca Raton: CRC Press; 1991. p. 1–43. ISBN: 9780849369629 - CAT# 6962. chp1
- [18] Christophorou LG. *Electron-Molecule Interactions and their Applications*. 1st ed. Orlando: Academic Press; 1984. DOI: 10.1109/TDEI.2010.5492245
- [19] Massey HSW. *Negative Ions*. 5th ed. London: Cambridge University Press; 1976. ISBN: 978-0-521-20775-1
- [20] Palmer RE, Rous P. Resonances in electron-scattering by molecules on surface. *Rev. Mod. Phys.* 1992; 64: 383–479. DOI: 10.1103/RevModPhys.64.383
- [21] Sanche L, Electron resonances in desorption induced by electronic transitions. *Surf. Sci.* 2000; 451: 82–90. DOI: 10.1016/S0039-6028(00)00011-X
- [22] O'Malley TE. Theory of dissociative attachment. *Phys. Rev.* 1966; 150: 1429. DOI: 10.1103/PhysRev.150.14
- [23] Shimamura I, Takayanagi K. *Electron-Molecule Collisions*. 1st ed. New York: Plenum Press; 1984. DOI: 10.1103/RevModPhys.52.29
- [24] Hinze J. *Electron-Atom and Electron-Molecule Collisions*. 1st ed. New York: Plenum Press; 1983. DOI: 10.1007/978-1-4899-2148-2
- [25] Christophorou LG. The lifetime of metastable negative ions. *Adv. Electron. Electron Phys.* 1978; 46: 55–129. DOI: 10.1016/S0065-2539(08)60411-4
- [26] Illenberger E, Momigny J. *Gaseous Molecular Ions: An Introduction to Elementary Processes Induced by Ionization*. 1st ed. New York: Springer Science & Business Media; 1992. DOI: 10.1007/978-3-662-07383-4
- [27] Zangwill A. *Physics at Surfaces*. 1st ed. Cambridge: Cambridge University Press; 1988. DOI: 10.1017/CBQ9780511622564
- [28] Sanche L, Michaud M. Interaction of low-energy electrons (1–30 eV) with condensed molecules: II. Vibrational-librational excitation and shape resonances in thin N₂ and CO films. *Phys. Rev. B* 1984; 30: 6078–6092. DOI: 10.1103/PhysRevB.30.6078

- [29] Fano U, Stephens JA. Slow electrons in condensed matter. *Phys. Rev. B* 1986; 34: 438. DOI: 10.1103/PhysRevB.34.438
- [30] Liljequist D. A model calculation of coherence effects in the elastic backscattering of very low energy electrons (1–20 eV) from amorphous ice. *Int. J. Radiat. Biol.* 2012; 88: 50–53. DOI: 10.3109/09553002.2011.577506
- [31] Michaud M, Bazin M, Sanche L. Measurement of inelastic cross sections for low-energy electron scattering from DNA bases. *Int. J. Radiat. Biol.* 2012; 88: 15–21. DOI: 10.3109/09553002.2011.577505
- [32] Michaud M, Wen A, Sanche L. Cross sections for low-energy (1–100 eV) electron elastic and inelastic scattering in amorphous ice. *Radiat. Res.* 2003; 159: 3–22. DOI: 0033-7587/03
- [33] Liljequist D. A study of errors in trajectory simulation with relevance for 0.2–50 eV electrons in liquid water. *Radiat. Phys. Chem.* 2008; 77: 835–853. DOI: 10.1016/j.radphyschem.2008.03.004
- [34] Toburen LH. Challenges in Monte Carlo track structure modelling. *Int. J. Radiat. Biol.* 2012; 88: 2–9. DOI:10.3109/09553002.2011.574781
- [35] Sanche L. Nanoscale dynamics of radiosensitivity: role of low energy electrons. In: Gomez-Tejedor GG, Fuss MC (eds). *Radiation Damage in Biomolecular Systems*. 1st ed. New York: Springer Science & Business Media; 2012. p. 3–43. DOI: 10.1007/978-94-007-2564-5. ch1
- [36] Keszei E, Jay-Gerin J-P, Perluzzo G, Sanche L. Quasielastic hot electron transport in solid N₂ films. *J. Chem. Phys.* 1986; 85: 7396–7402. DOI: 10.1063/1.451328
- [37] Sanche L, Bass AD, Ayotte P, Fabrikant II. Effect of the condensed phase on dissociative electron attachment: CH₃Cl condensed on a Kr surface. *Phys. Rev. Lett.* 1995; 75: 3568. DOI: 10.1103/PhysRevLett.75.3568
- [38] Michaud M, Sanche L. The 2Π_g shape resonance of N₂ near a metal surface and in rare gas solids. *J. Electron Spectrosc. Relat. Phenom.* 1990; 51: 237–248. DOI: 10.1016/0368-2048(90)80155-4
- [39] Sanche L. Low energy electron-driven damage in biomolecules. *Eur. Phys. J. D.* 2005; 35: 367–390. DOI: 10.1140/epjd/e2005-00206-6
- [40] Abdoul-Carime H, Gholke S, Illenberger E. Site-specific dissociation of DNA bases by slow electrons at early stage of irradiation. *Phys. Rev. Lett.* 2004; 92: 168103. DOI: 10.1103/PhysRevLett.92.168103
- [41] Ptasińska S, Denifl S, Grill V, Märk TD, Illenberger E, Scheier P. Bond- and site-selective loss of H⁻ from pyrimidine bases. *Phys. Rev. Lett.* 2005; 95: 093201. DOI: 10.1103/PhysRevLett.95.093201

- [42] Ptasińska S, Denifl S, Scheier P, Märk TD, Illenberger E. Bond and site selective loss of H atom from nucleobases by very low-energy electrons (<3 eV). *Angew. Chem. Int. Ed.* 2005; 44: 6941–6943. DOI: 10.1002/anie.200502040
- [43] Denifl S, Sulzer P, Huber D, Zappa F, Probst M, Märk TD, Scheier P, Injan N, Limtrakul J, Abouaf R, Dunet H. Influence of functional groups on the site-selective dissociation of adenine upon low-energy electron attachment. *Angew. Chem. Int. Ed.* 2007; 46: 5238–5241. DOI: 10.1002/anie.200700032
- [44] Dawley MM, Tanzer M, Carmichael I, Denifl S, Ptasińska S. Dissociative electron attachment to the gas-phase nucleobase hypoxanthine. *J. Chem. Phys.* 2015; 142: 215101. DOI: 10.1016/j.ijms.2013.12.005
- [45] Ptasińska S, Denifl S, Scheier P, Märk TD, Gohlke S, Illenberger E. Decomposition of thymidine by low energy electrons: Implications for the molecular mechanisms of single strand breaks in DNA. *Angew. Chem. Int. Ed.* 2006; 45: 1893–1896. DOI: 10.1002/anie.200503930
- [46] Burrow PD, Gallup GA, Scheer AM, Denifl S, Ptasińska S, Märk TD, Scheier P. Vibrational Feshbach resonances in uracil and thymine. *J. Chem. Phys.* 2006; 124: 124310. DOI: 10.1063/1.2181570
- [47] Gallup GA, Fabrikant II. Vibrational Feshbach resonances in dissociative electron attachment to uracil. *Phys. Rev. A* 2011; 83: 012706. DOI: 10.1103/PhysRevA.84.012701
- [48] Francés-Monerris A, Segarra-Martí J, Merchán M, Roca-Sanjuán D. Complete-active-space second-order perturbation theory (CASPT2//CASSCF) study of the dissociative electron attachment in canonical DNA nucleobases caused by low-energy electrons (0–3 eV). *J. Chem. Phys.* 2015; 143: 215101. DOI: 10.1063/1.4936574
- [49] Ferreira da Silva F, Matias C, Almeida D, García G, Ingólfsson O, Dögg Flosadóttir O, Ómarsson B, Ptasińska S, Puschnigg B, Scheier P, Limão-Vieira P, Denifl S. NCO^- , a key fragment upon dissociative electron attachment and electron transfer to pyrimidine bases: site selectivity for a slow decay process. *J. Am. Soc. Mass Spectrom.* 2013; 24: 1787–1797. DOI: 10.1007/s13361-013-0715-9
- [50] Aflatooni K, Scheer AM, Burrow PD. Total dissociative electron attachment cross sections for molecular constituents of DNA. *J. Chem. Phys.* 2006; 125: 054301. DOI: 10.1063/1.2229209
- [51] Ptasińska S, Denifl S, Scheier P, Märk TD. Inelastic electron interaction (attachment/ionization) with deoxyribose. *J. Chem. Phys.* 2004; 120: 8505–8511. DOI: 10.1063/1.1690231
- [52] Ibanescu BC, May O, Monney A, Allan M. Electron induced chemistry of alcohols. *Phys. Chem. Chem. Phys.* 2007; 9: 3163–3173. DOI: 10.1039/B704656A

- [53] Fujita T, Kondo M, Takayanagi T. Quantum chemical study of dissociative electron attachment to D-ribose and D-fructose. *Comp. Theor. Chem.*. 2016; 1075: 70–76. DOI: 10.1140/epjd/e2005-00206-6
- [54] Sommerfeld T, Doorway mechanism for dissociative electron attachment to fructose. *J. Chem. Phys.* 2007; 126: 124301. DOI: 10.1063/1.2710275
- [55] Baccarelli I, Gianturco FA, Grandi A, Sanna N, Lucchese RR, Bald I, Kopyra J, Illenberger E. Selective bond breaking in β -D-ribose by gas-phase electron attachment around 8 eV. *J. Am. Chem. Soc.* 2007; 129: 6269–6277. DOI: 10.1021/ja070542h
- [56] Kopyra J. Low energy electron attachment to the nucleotide deoxycytidine monophosphate: direct evidence for the molecular mechanisms of electron-induced DNA strand breaks. *Phys. Chem. Chem. Phys.* 2012; 14: 8287–8289. DOI: 10.1039/c2cp40847c
- [57] König C, Kopyra J, Bald I, Illenberger E. Dissociative electron attachment to phosphoric acid esters: the direct mechanism for single strand breaks in DNA. *Phys. Rev. Lett.* 2006; 97: 018105. DOI: 10.1103/PhysRevLett.97.018105
- [58] Abouaf R, Dunet H. Structures in dissociative electron attachment cross-sections in thymine, uracil and halouracils. *Eur. Phys. J. D.* 2005; 35: 405–410. DOI: 10.1140/epjd/e2005-00239-9
- [59] Abdoul-Carime H, Huels MA, Illenberger E, Sanche L. Formation of negative ions from gas phase halo-uracils by low-energy (0–18 eV) electron impact. *Int. J. Mass Spectrom.* 2003; 228: 703–716. DOI: 10.1016/S1387-3806(03)00139-8
- [60] Abouaf R, Pommier J, Dunet H. Negative ions in thymine and 5-bromouracil produced by low energy electrons. *Int. J. Mass Spectrom.* 2003; 226: 397–403. DOI: 10.1016/S1387-3806(03)00085-X
- [61] Scheer AM, Aflatooni K, Gallup GA, Burrow PD. Bond breaking and temporary anion states in uracil and halouracils: implications for the DNA bases. *Phys. Rev. Lett.* 2004; 92: 068102. DOI: 10.1103/PhysRevLett.92.068102
- [62] Kossoski F, do N. Varella MT. Negative ion states of 5-bromouracil and 5-iodouracil. *Phys. Chem. Chem. Phys.* 2015; 17: 17271. DOI: 10.1039/C5CP01475A
- [63] Denifl S, Candori P, Ptasińska S, Limão-Vieira P, Grill V, Märk TD, Scheier P. Positive and negative ion formation via slow electron collisions with 5-bromouridine. *Eur. Phys. J. D.* 2005; 35: 391–398. DOI: 10.1140/epjd/e2005-00205-7
- [64] Denifl S, Matejčík S, Gstir B, Hanel G, Probst M, Scheier P, Märk TD. Electron attachment to 5-chloro uracil. *J. Chem. Phys.* 2003; 118: 4107. DOI: 10.1063/1.1540108
- [65] Kossoski F, Bettega MHF, do N. Varella MT. Shape resonance spectra of uracil, 5-fluorouracil, and 5-chlorouracil. *J. Chem. Phys.* 2014; 140: 024317. DOI: 10.1063/1.4861589

- [66] Denifl S, Matejcek S, Ptasińska S, Gstir B, Probst M, Scheier P, Illenberger P, Märk TD. Electron attachment to chlorouracil: a comparison between 6-CIU and 5-CIU. *J. Chem. Phys.* 2004; 120: 704–709. DOI: 10.1063/1.1630959
- [67] Modelli A, Bolognesi P, Avaldi L. Temporary anion states of pyrimidine and halopyrimidines. *J. Phys. Chem. A.* 2011; 115: 10775–10782. DOI: 10.1021/jp206559d
- [68] Kossoski F, Kopyra J, do N. Varella MT. Anion states and fragmentation of 2-chloroadenine upon low-energy electron collisions. *Phys. Chem. Chem. Phys.* 2015; 17: 28958–28965. DOI: 10.1039/C5CP04967A
- [69] Kopyra J, Keller A, Bald I. On the role of fluoro-substituted nucleotides in DNA radiosensitization for tumor radiation therapy. *RSC Adv.* 2014; 4: 6825–6829. DOI: 10.1039/C3RA46735J
- [70] Abouaf R, Ptasińska S, Teillet-Billy D. Low energy electron impact on gas phase 5-nitrouracil. *Chem. Phys. Lett.* 2008; 455: 169–173. DOI: 10.1016/j.cplett.2008.02.104
- [71] Ptasińska S, Alizadeh E, Sulzer P, Abouaf R, Mason NJ, Märk TD, Scheier P. Negative ion formation by low energy electron attachment to gas phase 5-nitrouracil. *Int. J. Mass Spectrom.* 2008; 277: 291–295. DOI: 10.1016/j.ijms.2008.06.008
- [72] Tanzer K, Feketeova L, Puschnigg B, Scheier P, Illenberger E, Denifl S. Reactions in nitroimidazole and methylnitroimidazole triggered by low-energy (0–8 eV) electrons. *J. Phys. Chem. A.* 2014; 119: 6668–6675. DOI: 10.1021/acs.jpca.5b02721
- [73] Tanzer K, Feketeova L, Puschnigg B, Scheier P, Illenberger E, Denifl S. Reactions in nitroimidazole triggered by low-energy (0–2 eV) electrons: methylation at N1-H completely blocks reactivity. *Angew. Chem. Int. Ed.* 2015; 53: 12240–12243. DOI: 10.1002/anie.201407452
- [74] Tanzer K, Pelc A, Huber SE, Smialek MA, Scheier P, Probst M, Denifl S. Low energy electron attachment to platinum(II) bromide (PtBr₂). *Int. J. Mass Spectrom.* 2014; 365: 152–156. DOI: 10.1016/j.ijms.2013.11.016
- [75] Glick BR, Pasternak JJ, Patten CL. *Molecular Biotechnology: Principles and Applications of Recombinant DNA.* 4th ed. Washington: ASM Science; 2010. DOI: 10.1128/9781555816124
- [76] Boulanouar O, Fromm M, Mavon C, Cloutier P, Sanche L. Dissociative electron attachment to DNA-diamine thin films: impact of the DNA close environment on the OH and O decay channels. *J. Chem. Phys.* 2013; 139: 055101. DOI: 10.1063/1.4815967
- [77] Zheng Y, Cloutier P, Hunting DJ, Sanche L, Wagner JR. Chemical basis of DNA sugar-phosphate cleavage by low-energy electrons. *J. Am. Chem. Soc.* 2005; 127: 16592–16598. DOI: 10.1021/ja054129q

- [78] Zheng Y, Wagner JR, Sanche L. DNA damage induced by low-energy electrons: electron transfer and diffraction. *Phys. Rev. Lett.* 2006; 96: 208101. DOI: 10.1103/PhysRevLett.96.208101
- [79] Zheng Y, Cloutier P, Hunting DJ, Wagner JR, Sanche L. Phosphodiester and N-glycosidic bond cleavage in DNA induced by 4–15 eV electrons. *J. Chem. Phys.* 2006; 124: 064710. DOI: 10.1063/1.2166364
- [80] Keller A, Bald I, Rotaru A, Cauët E, Gothelf CV, Besenbacher F. Probing Electron-induced bond cleavage at the single-molecule level using DNA origami templates. *ACS Nano* 2012; 6: 4392-4399. DOI: 10.1021/nn3010747
- [81] Keller A, Kopyra J, Gothelf KV, Bald I. Electron-induced damage of biotin studied in the gas phase and in the condensed phase at a single-molecule level. *New J. Phys.* 2013; 15: 083045. DOI: 10.1088/1367-2630/15/8/083045
- [82] Bald I, Keller A. Molecular processes studied at a single-molecule level using DNA origami nanostructures and atomic force microscopy. *Molecules* 2014; 19: 13803–13823. DOI: 10.3390/molecules190913803
- [83] Park Y, Polska K, Rak J, Wagner JR, Sanche L. Fundamental mechanisms of DNA radiosensitization: damage induced by low-energy electrons in brominated oligonucleotide trimers. *J. Phys. Chem. B* 2012; 116: 9676–9682. DOI: 10.1021/jp304964r
- [84] Panajotovic R, Martin F, Cloutier P, Hunting DJ, Sanche L. Effective cross sections for production of single-strand breaks in plasmid DNA by 0.1 to 4.7 eV electrons. *Radiat. Res.* 2006; 165: 452–459. DOI: 10.1667/RR3521.1
- [85] Boulanouar O, Fromm M, Bass AD, Cloutier P, Sanche L. Absolute cross section for loss of supercoiled topology induced by 10 eV electrons in highly uniform/DNA/1,3-diaminopropane films deposited on highly ordered pyrolytic graphite. *J. Chem. Phys.* 2013; 139: 5. DOI: 10.1063/1.4817323
- [86] Keller A, Rackwitz J, Cauët E, Liévin J, Körzdörfer T, Rotaru A, Gothelf KV, Besenbacher F, Bald I. Sequence dependence of electron-induced DNA strand breakage revealed by DNA nanoarrays. *Sci. Rep.* 2014; 4: 7391. DOI: 10.1038/srep07391
- [87] Huels M, Boudaïffa B, Cloutier P, Hunting DJ, Sanche L. Single, double, and multiple double strand breaks induced in DNA by 3-100 eV electrons. *J. Am. Chem. Soc.* 2003; 125: 4467–4477. DOI: 10.1021/ja029527x
- [88] Von Sonntag C. *The Chemical Basis of Radiation Biology*. 1st ed. London: Taylor and Francis; 1987. DOI: 10.1016/1011-1344(89)80053-3
- [89] Podhorecka M, Skladanowski A, Bozko P. H2AX phosphorylation: its role in DNA damage response and cancer therapy. *J. Nucl. Acids.* 2010; 2010: 920161. DOI: 10.4061/2011/920161

- [90] Martin F, Burrow PD, Cai Z, Cloutier P, Hunting DJ, Sanche L. DNA strand breaks induced by 0-4 eV electrons: The role of shape resonances. *Phys. Rev. Lett.* 2004; 93: 068101. DOI: 10.1103/PhysRevLett.93.068101
- [91] Li X, Sevilla MD, Sanche L. Density functional theory studies of electron interaction with DNA: can zero eV electrons induce strand breaks? *J. Am. Chem. Soc.* 2003; 125: 13668–13669. DOI: 10.1021/ja036509m
- [92] Simons J. How do low-energy (0.1-2 eV) electrons cause DNA-strand breaks? *Acc. Chem. Res.* 2006; 39: 772–779. DOI: 10.1021/ar0680769
- [93] Bao X, Wang J, Gu J, Leszczynski J. DNA strand breaks induced by near-zero-electron-volt electron attachment to pyrimidine nucleotides. *PNAS* 2006; 103: 5658–5663. DOI: 10.1073/pnas.0510406103
- [94] Caron LG, Sanche L. Diffraction in resonant electron scattering from helical macromolecules: A- and B-type DNA. *Phys. Rev. A: At. Mol. Opt. Phys.* 2004; 70: 032719. DOI: 10.1103/PhysRevA.70.032719
- [95] Caron LG, Sanche L. Theoretical studies of electron interactions with DNA and its subunits: from tetrahydrofuran to plasmid DNA. In: Čársky P, Čurík R (eds). *Low-energy Electron Scattering from Molecules, Biomolecules and Surfaces*. 1st ed. Boca Raton: CRC Press (Taylor and Francis Group); 2012. p. 161–230. ISBN: 978-1-4398-3910-2. Ch. 6.
- [96] Gu J, Leszczynski J, Schaefer III F. Interactions of electrons with bare and hydrated biomolecules: from nucleic acid bases to DNA segments. *Chem Rev.* 2012; 112: 5603–5640. DOI: 10.1021/cr3000219
- [97] Sidorov AN, Orlando TM. Monolayer graphene platform for the study of DNA damage by low-energy electron irradiation. *Phys. Chem. Lett.* 2013; 4: 2328–2333. DOI: 10.1021/jz4010416
- [98] Han X, Klas M, Liu Y, Stack MS, Ptasinska S. DNA damage in oral cancer cells induced by nitrogen atmospheric pressure plasma jets. *Appl. Phys. Lett.* 2013; 102: 233703. DOI: 10.1063/1.4809830
- [99] Dame RT. The role of nucleoid-associated proteins in the organization and compaction of bacterial chromatin. *Mol. Microbiol.* 2005; 56: 858–870. DOI: 10.1111/j.1365-2958.2005.04598.x
- [100] Mehmood S, Allison TM, Robinson CV. Mass spectrometry of protein complexes: from origins to applications. *Ann. Rev. Phys. Chem.* 2015; 66: 453–474. DOI: 10.1146/annurev-physchem-040214-121732
- [101] Lin SD. Electron radiation damage of thin films of glycine, diglycine, and aromatic amino acids. *Radiat. Res.* 1974; 59: 521–536. DOI: 10.2307/3574071

- [102] Abdoul-Carime H, Cecchini S, Sanche L. Alteration of protein structure induced by low-energy (<18 eV) electrons: I. The peptide and disulfide bridges. *Radiat. Res.* 2002; 158: 23–31. DOI: 10.1016/j.mrfmmm.2009.06.016
- [103] Abdoul-Carime H, Sanche L. Alteration of protein constituents induced by low energy (<35 eV) electrons: II. Dissociative electron attachment to amino acids containing cyclic groups. *Radiat. Res.* 2003; 160: 86–94. DOI: 10.1039/b814219j
- [104] Karas M, Hillenkamp F. Laser desorption ionization of proteins with molecular masses exceeding 10,000 Daltons. *Anal. Chem.* 1988; 60: 2299–2301. DOI: 10.1021/ac00171a028
- [105] Hillenkamp F, Karas M. Matrix-assisted laser desorption/ionisation, an experience. *Int. J. Mass Spectrom.* 2000; 200: 71–77. DOI: 10.1111/j.1469-0691.2010.03274.x
- [106] Karas M, Bahr U, Fournier I, Glückmann M, Pfenninger A. The initial ion velocity as a marker for different desorption-ionization mechanisms in MALDI. *Int. J. Mass Spectrom.* 2003; 226: 239–248. DOI: 10.1016/S1387-3806(02)01062-X
- [107] Wind M, Lehmann W. Element and molecular mass spectrometry—An emerging analytical dream team in the life sciences. *J. Anal. At. Spectrom.* 2004; 19: 20–25. DOI: 10.1039/B309482K
- [108] Brøndsted Nielsen S, Andersen JU, Hvelplund P, Liu B, Tomita S. Biomolecular ions in accelerators and storage rings. *J. Phys. B: At. Mol. Opt. Phys.* 2004; 37: R25–R56. DOI: 10.1088/0953-4075/37/8/R01
- [109] Fenn JB, Mann M, Meng CK, Wong SF, Whitehouse CM. Electrospray ionization for mass spectrometry of large biomolecules. *Science* 1989; 246: 64–71. DOI: 10.1126/science.2675315
- [110] Lucas B, Grégoire G, Lemaire J, Maître P, Ortega JM, Rupenyan A, Reimann B, Schermann JP, Desfrancois C. Investigation of the protonation site in the dialanine peptide by infrared multiphoton dissociation spectroscopy. *Phys. Chem. Chem. Phys.* 2004; 6: 2659–2663. DOI: 10.1039/B316053J
- [111] Laskin J, Denisov E, Futrell JH. A comparative study of collision-induced and surface-induced dissociation. 1. Fragmentation of protonated dialanine. *J. Am. Chem. Soc.* 2000; 122: 9703–9714. DOI: 10.1021/ja001384w
- [112] Polce MJ, Ren D, Wesdemiotis C. Dissociation of the peptide bond in protonated peptides. *Int. J. Mass Spectrom.* 2000; 35: 1391–1398. DOI: 10.1002/1096-9888(200012)35:12
- [113] Laskin J, Futrell JH. On the efficiency of energy transfer in collisional activation of small peptides. *J. Chem. Phys.* 2002; 116: 4302–4310. DOI: 10.1016/S1387-3806(02)01017-5
- [114] Wang J, Meroueh SO, Wang Y, Hase WL. Efficiency of energy transfer in protonated diglycine and dialanine SID: Effects of collision angle, peptide ion size, and intramolecular potential. *Int. J. Mass Spectrom.* 2003; 230: 57–63. DOI: 10.1016/j.ijms.2003.08.005

- [115] Ptasińska S, Denifl S, Candor P, Matejcik S, Scheier P, Märk TD. Dissociative electron attachment to gas phase alanine. *Chem. Phys. Lett.* 2005; 403: 107–112. DOI: 10.1016/j.cplett.2004.12.115
- [116] Abdoul-Carime H, Gohlke S, Illenberger E. Fragmentation of tryptophan by low-energy electrons. *Chem. Phys. Lett.* 2005; 402: 497–502. DOI: 10.1016/j.cplett.2004.12.073
- [117] Gohlke S, Rosa A, Illenberger E, Brüning F, Huels MA. Formation of anion fragments from gas-phase glycine by low energy (0–15 eV) electron impact. *J. Chem. Phys.* 2002; 116: 10164–10169. DOI: 10.1063/1.1479348
- [118] Ptasińska S, Denifl S, Abedi A, Scheier P, Märk TD. Dissociative electron attachment to gas-phase glycine. *Anal. Bioanal. Chem.* 2003; 377: 1115–1119. DOI: 10.1007/s00216-003-2254-x
- [119] Abdoul-Carime H, Illenberger E. Fragmentation of proline induced by slow electrons. *Chem. Phys. Lett.* 2004; 397: 309–313. DOI: 10.1016/j.cplett.2004.08.119
- [120] Sulzer P, Alizadeh E, Mauracher A, Scheier P, Märk TD. Detailed dissociative electron attachment studies on the amino acid proline. *Int. J. Mass. Spectrom.* 2008; 277: 274–278. DOI:10.1016/j.ijms.2009.10.003
- [121] Abdoul-Carime, H.; Gohlke, S.; Illenberger, E. Conversion of amino-acids by electrons at subexcitation energies. *Phys. Chem. Chem. Phys.* 2004; 6: 161–164. DOI: 10.1039/B311675A
- [122] Alizadeh, E. Dissociative Electron Attachment to Biomolecules [thesis], Innsbruck: University of Innsbruck; 2009.
- [123] Kocisek J, Papp P, Mach P, Vasil'ev YV, Deinzer ML, Matejcik S. Resonance electron capture by serine. *J. Phys. Chem. A* 2010; 114: 1677–1683. DOI: 10.1021/jp906636b
- [124] Alizadeh E, Gschliesser D, Bartl P, Edtbauer A, Vizcaino V, Mauracher A, Probst M, Märk TD, Ptasińska S, Mason NJ, Denifl S, Scheier P. Bond dissociation of the dipeptide dialanine and its derivative alanine anhydride induced by low energy electrons. *J. Chem. Phys.* 2011; 134: 054305. DOI: 10.1063/1.3544217
- [125] Vasil'ev YV, Figard BJ, Barofsky DF, Deinzer ML. Resonant electron capture by some amino acids esters. *Int. J. Mass Spectrom.* 2007; 268: 106–121. DOI: 10.1016/j.ijms.2007.07.006
- [126] Gallup GA, Burrow PD, Fabrikant II. Electron-induced bond breakage at low energies in HCOOH and glycine: the role of very short-lived short-lived σ^* anion states. *Phys. Rev. A* 2009; 79: 042701. DOI: 10.1103/PhysRevA.79.042701
- [127] Abdoul-Carime H, König-Lehmann C, Kopyra J, Farizon B, Farizon M, Illenberger E. Dissociative electron attachment to amino-acids: the case of leucine. *Chem. Phys. Lett.* 2009; 477: 245–248. DOI:10.1016/j.cplett.2009.07.021

- [128] Abdoul-Carime H, Sanche, L. Alteration of protein constituents induced by low-energy (<40 eV) electrons. III. The aliphatic amino acids. *J. Phys. Chem. B* 2004; 108: 457–464. DOI: 10.1021/jp030413x
- [129] Cloutier P, Sicard-Roselli C, Escher E, Sanche L. Low-energy (3–24 eV) electron damage to the peptide backbone. *J. Phys. Chem. B* 2007; 111: 1620–1624. DOI: 10.1021/jp066947q
- [130] Uvdal K, Bodo P, Liedberg B. l-cysteine adsorbed on gold and copper: An X-ray photoelectron spectroscopy study. *J. Colloid Interface Sci.* 1992; 149: 162–173. DOI: 10.1016/0021-9797(92)90401-7
- [131] Kühnle A, Linderoth TR, Hammer B, Besenbacher F. Chiral recognition in dimerization of adsorbed cysteine observed by scanning tunnelling microscopy. *Nature* 2002; 415: 891–893. DOI: 10.1021/nn9012803
- [132] L. Buimaga-Iarinca L, Calborean A. Electronic structure of the ll-cysteine dimers adsorbed on Au(111): a density functional theory study. *Phys. Scr.* 2012; 86: 035707. DOI:10.1088/0031-8949/86/03/035707
- [133] Jain PK, Qian W, El-Sayed MA. Ultrafast cooling of photoexcited electrons in gold nanoparticle-thiolated DNA conjugates involves the dissociation of the gold-thiol bond. *J. Am. Chem. Soc.* 2006; 128: 2426–2433. DOI: 10.1021/ja056769z
- [134] Alizadeh E, Massey S, Rowntree PA, Sanche L. Low-energy electron-induced dissociation in condensed-phase L-cysteine I: desorption of anions from chemisorbed films. *J. Phys.: Conf. Ser.* 2015; 635: 012001. DOI: 10.1088/1742-6596/635/1/012001
- [135] Alizadeh E, Massey S, Sanche L, Rowntree PA. Low-energy electron-induced dissociation in condensed-phase L-cysteine II: a comparative study on desorption from chemisorbed and physisorbed films. *Eur. Phys. J. D* 2016; 70: 1–8 DOI: 10.1140/epjd/e2016-60739-y
- [136] Solomun T, Skalicky T. The interaction of a protein-DNA surface complex with low-energy electrons. *Chem. Phys. Lett.* 2008; 453: 101–104. DOI: 10.1016/j.cplett.2007.12.078
- [137] Ptasińska S, Li Z, Mason NJ, Sanche L. Damage to amino acid–nucleotide pairs induced by 1 eV electrons. *Phys. Chem. Chem. Phys.* 2010; 12: 9367–9372. DOI: 10.1039/B926267A
- [138] Wang J, Gu J, Leszczynski J. Electron detachment of the hydrogen-bonded amino acid side-chain–guanine complexes. *Chem. Phys. Lett.* 2007; 442: 124–127. DOI: 10.1016/j.cplett.2007.05.071
- [139] Gu B, Smyth M, Kohanoff J. Protection of DNA against low-energy electrons by amino acids: a first-principles molecular dynamics study. *Phys. Chem. Chem. Phys.* 2014; 16: 24350–24358. DOI: 10.1039/C4CP03906H
- [140] Ptasińska S, Sanche L. Dissociative electron attachment to hydrated single DNA strands. *Phys. Rev. E* 2007; 75: 031915. DOI: 10.1103/PhysRevE.75.031915

- [141] Falk M, Hartman KA, Lord RC. Hydration of deoxyribonucleic acid. II. An infrared study. *J. Am. Chem. Soc.* 1963; 85: 387–391. DOI: 10.1021/ja00887a004
- [142] Orlando TM, Oh D, Chen Y, Alexandrov A. Low-energy electron diffraction and induced damage in hydrated DNA. *J. Chem. Phys.* 2008; 128: 195102. DOI: 10.1063/1.2907722
- [143] Grieves GA, McLain JL, Orlando TM. Low-energy electron-stimulated reactions in nanoscale water films and water-DNA interfaces. In: Hatano Y, Katsumura Y, Mozumder A (eds). *Charged Particle and Photon Interactions with Matter, Recent Advances, Applications, and Interfaces*. 1st ed. Boca Raton: CRC Press; 2011. p 473–501. ISBN 9781439811771. Ch. 18.
- [144] Sidorov AN, Orlando TM. Monolayer graphene platform for the study of DNA damage by low-energy electron irradiation. *Phys. Chem. Lett.* 2013; 4: 2328–2333. DOI: 10.1021/jz4010416
- [145] Alizadeh E, Cloutier P, Hunting DJ, Sanche L. Soft X-ray and low energy electron-induced damage to DNA under N₂ and O₂ atmospheres. *J. Phys. Chem. B* 2011; 115: 4523–4531. DOI: 10.1021/jp200947g
- [146] Alizadeh E, Sanche L. The role of humidity and oxygen level on damage to DNA induced by soft X-rays and low-energy electrons. *J. Phys. Chem. C* 2013; 117: 22445–22453. DOI: 10.1021/jp403350j
- [147] Alizadeh E, Sanz AG, Madugundu GS, Garcia G, Wagner JR, Sanche L. Thymidine decomposition induced by low-energy electrons and soft X-rays under N₂ and O₂ atmospheres. *Radiat. Res.* 2014; 181: 629–640. DOI: 10.1667/RR13584.1
- [148] Gokhberg K, Kolorenč P, Kuleff AI, Cederbaum LS. Site- and energy-selective slow-electron production through intermolecular Coulombic decay. *Nature* 2014; 505: 661–663. DOI: 10.1038/nature12927
- [149] Cederbaum LS, Zobeley J, Tarantelli F. Giant intermolecular decay and fragmentation of clusters. *Phys. Rev. Lett.* 1997; 79: 4778–4781. DOI: 10.1103/PhysRevLett.79.4778.
- [150] Santra R, Zobeley J, Cederbaum LS, Moiseyev N. Interatomic coulombic decay in van der Waals clusters and impact of nuclear motion. *Phys. Rev. Lett.* 2000; 85: 4490–4493. DOI: 10.1103/PhysRevLett.85.4490
- [151] Grieves GA, Orlando TM. Intermolecular coulomb decay at weakly coupled heterogeneous interfaces. *Phys. Rev. Lett.* 2011; 107: 016104. DOI: 10.1103/PhysRevLett.107.016104
- [152] Mucke M, Braune M, Barth S, Förstel M, Lischke T, Ulrich V, Arion T, Becker U, Bradshaw A, Hergenhan U. A hitherto unrecognized source of low-energy electrons in water. *Nat. Phys.* 2010; 6: 143–146. DOI: 10.1038/nphys1500

- [153] Hergenhan U. Production of low kinetic energy electrons and energetic ion pairs by intermolecular Coulombic decay. *Int. J. Radiat. Biol.* 2012; 88: 871–883. DOI: 10.3109/09553002.2012.698031
- [154] Kouass Sahbani S, Sanche L, Cloutier P, Bass AD, Hunting DJ. Loss of cellular transformation efficiency induced by DNA irradiation with low-energy (10 eV) electrons. *J. Phys. Chem. B* 2014; 118:13123–13131. DOI: 10.1021/jp508170c
- [155] Boulanouar O, Khatyr A, Herlem G, Palmino F, Sanche L, Fromm M. Soft adsorption of densely packed layers of DNA-plasmid•1,3-diaminopropane complexes onto highly oriented pyrolytic graphite designed to erode in water. *J. Phys. Chem. C* 2011; 115: 21291–21298. DOI: 10.1021/jp207083r
- [156] Kouass Sahbani S, Sanche L, Cloutier P, Bass AD, Hunting DJ. Electron resonance decay into a biological function: decrease in viability of *E. coli* transformed by plasmid DNA irradiated with 0.5–18 eV electrons. *J. Phys. Chem. Lett.* 2015; 6: 3911–3914. DOI: 10.1021/acs.jpcllett.5b01585
- [157] Dugal P-C, Abdoul-Carime H, Sanche L. Mechanisms of low energy (0.5–30 eV) electron-induced pyrimidine ring fragmentation within thymine and halogen-substituted single strands of DNA. *J. Phys. Chem. B.* 2000; 104: 5610–5617. DOI: 10.1021/jp9938112
- [158] Abdoul-Carime H, Dugal P-C, Sanche L. Damage induced by 1–30 eV electrons on thymine and bromouracil substituted oligonucleotides. *Radiat. Res.* 2000; 153: 23–28. DOI: 10.1667/0033-7587(2000)153
- [159] Abouaf R, Pommier J, Dunet H. Electronic and vibrational excitation in gas phase thymine and 5-bromouracil by electron impact. *Chem. Phys. Lett.* 2003; 381: 486–494. DOI: 10.1016/j.cplett.2003.09.121
- [160] Klyachko DV, Huels MA, Sanche L. Halogen anion formation in 5-halouracil films: X-rays vs subionization electrons. *Radiat. Res.* 1999; 151: 177–187. DOI: 10.2307/3579945
- [161] Li Z, Cloutier P, Sanche L, Wagner JR. Low energy electron induced DNA damage in a trinucleotide containing 5-bromouracil. *J. Phys. Chem. B.* 2011; 115: 13668–13673. DOI: 10.1021/jp205428j
- [162] Abdoul-Carime H, Limao-Vieira P, Gohlke S, Petrushko I, Mason NJ, Illenberger E. Sensitization of 5-bromouridine by slow electrons. *Chem. Phys. Lett.* 2004; 393: 442–447. DOI: 10.1016/j.cplett.2004.06.081
- [163] du Penhoat H, Huels MA, Cloutier P, Jay-Gerin J-P, Sanche L. Electron stimulated desorption of H- from thin films of 5-halouracils. *Phys. Chem.* 2003; 5: 3270–3277. DOI: 10.1039/B212552H
- [164] du Penhoat H, Huels MA, Cloutier P, Jay-Gerin J-P, Sanche L. Anion fragment formation in 5-halouracil films induced by 1–20 eV electron impact. *J. Phys. Chem. B* 2004; 108: 17251–17260. DOI: 10.1021/jp0478817

- [165] Li X, Sanche L, Sevilla MD. Dehalogenation of 5-halouracils after low energy electron attachments: a density functional theory investigation. *J. Phys. Chem. A*. 2002; 106: 11248–11253. DOI: 10.1021/ja034286u
- [166] Park Y, Polska K, Rak J, Wagner JR, Sanche L. Fundamental mechanisms of DNA radiosensitization: damage induced by low energy electrons in brominated oligonucleotide trimers. *J. Phys. Chem. B*. 2012; 116: 9676–9682. DOI: 10.1021/jp304964r
- [167] Polska K, Rak J, Bass AD, Cloutier P, Sanche L. Electron simulated desorption of anions from native and brominated single stranded oligonucleotide trimers. *J. Chem. Phys.* 2012; 136: 075101. DOI: 10.1063/1.3685587
- [168] Zimbrick JD, Ward JF, Myers LS. Studies on the chemical basis of cellular radiosensitization by 5-bromouracil substitution in DNA. *Int. J. Radiat. Biol.* 1969; 16: 505–523. DOI: 10.1080/09553006914551571
- [169] Tanzer K, Pelc A, Huber SE, Śmiałek MA, Scheier P, Probst M, Denifl S. Low energy electron attachment to platinum(II) bromide (PtBr₂). *Int. J. Mass Spectrom.* 2013; 365: 152–156. DOI: 10.1016/j.ijms.2013.11.016
- [170] Scheer AM, Aflatooni K, Gallup GA, Burrow PD. Bond breaking and temporary anion states in uracil and halouracils: implications for the DNA bases. *Phys. Rev. Lett.* 2004; 92: 068102. DOI: 10.1103/PhysRevLett.92.068102
- [171] Abdoul-Carime H, Dugal P. C, Sanche L. DIET of neutral fragments from chemisorbed biological molecular systems. *Surf. Sci.* 2000; 451: 102–107. DOI: 10.1016/S0039-028(00)00014-5
- [172] Cheng HY, Hsieh SH, Chen YC, Lin CJ, Liu WC. Temporary anion states of radiosensitive halopyrimidines: shape and core-excited resonances. *Comp. Theor. Chem.* 2016; 1075: 18–29. DOI: 10.1016/j.comptc.2015.10.031
- [173] Cecchini S, Girouard S, Huels MA, Sanche L, Hunting DJ. Single-strand-specific radiosensitization of DNA by bromodeoxyuridine. *Radiat. Res.* 2004; 162: 604–615. DOI: 10.1667/RR3267
- [174] Sevilla M. Research breakthrough: DNA strandedness controls halouracil radiosensitization. *Radiat. Res.* 2004; 162: 603–603. DOI:10.1140/epjd/e2005-00206-6
- [175] Zheng Y, Hunting DJ, Ayotte P, Sanche L. Role of secondary low-energy electrons in the concomitant chemoradiation therapy of cancer. *Phys. Rev. Lett.* 2008; 100: 198101. DOI: 10.1103/PhysRevLett.100.198101
- [176] Tannock IF. Treatment of cancer with radiation and drugs. *J. Clin. Oncol.* 1996; 14: 3156–3174. DOI: 10.1200/JCO.2015.635540
- [177] Prestwich RJ, Shaakespeare D, Waters S. The rationale for and the current role of chemoradiotherapy. *J. Radiother. Pract.* 2007; 6: 11–19. DOI: 10.1097/CND.0b013e3181629396

- [178] Rezaee M, Alizadeh E, Cloutier P, Hunting DJ, Sanche L. A single subexcitation-energy electron can induce a double strand break in DNA modified by platinum chemotherapeutic drugs. *Chem. Med. Chem.* 2014; 9: 1145–1149. DOI: 10.1002/cmdc.201300462
- [179] Rezaee M, Sanche L, Hunting DJ. Cisplatin enhances the formation of DNA single and double strand breaks by hydrated electrons and hydroxyl radicals. *Radiat. Res.* 2013; 179: 323–331. DOI: 10.1667/RR3185.1
- [180] Rezaee M, Hunting DJ, Sanche L. New insights into the mechanism underlying the synergistic action of ionizing radiation with platinum chemotherapeutic drugs: the role of low-energy electrons. *Int. J. Radiat. Oncol. Biol. Phys.* 2013; 87: 847–853. DOI: 10.1016/j.ijrobp.2013.06.2037
- [181] Behmand B, Wagner JR, Sanche L, Hunting DJ. Cisplatin intrastrand adducts sensitive DNA to base by hydrated electrons. *J. Phys. Chem. B.* 2014; 118: 4803–4808. DOI: 10.1021/jp5014913
- [182] Behmand B, Wagner J. R, Hunting D, Marignier JL, Mostafavi M, Sanche L. Rate constant of reaction between the GTG-cisplatin complex and hydrated electrons. *J. Phys. Chem. B.* 2015; 119: 9496–9500. DOI: 10.1021/acs.jpcc.5b01752
- [183] Luo X, Zheng Y, Sanche L. DNA strand breaks and crosslinks induced by transient anions in the electron-energy range 2-20 eV. *J. Chem. Phys.* 2014; 140: 155101. DOI: 10.1063/1.4870519
- [184] Bao Q, Chen Y, Zheng Y, Sanche L. Cisplatin radiosensitization of DNA irradiated with 2-20 eV electrons: role of transient anions. *J. Phys. Chem. C.* 2014; 118: 15516–15524. DOI: 10.1021/jp503706h
- [185] Tippayamontri T, Kotb R, Paquette B, Sanche L. Optimal timing in concomitant chemoradiation therapy of colorectal tumors in nude mouse treated with Cisplatin and Lipoplatin™. *Anticancer Res.* 2013; 33: 3005–3014. DOI: 10.1155/2013/409179
- [186] Tippayamontri T, Kotb R, Sanche L, Paquette B. New therapeutic possibilities of combined treatment of radiotherapy with oxaliplatin and its liposomal formulations Lipoxal™ in rectal cancer using nude mouse xenograft. *Anticancer Res.* 2014; 34: 5303–5312.
- [187] Boulikas T, Vougiouka M. Cisplatin and platinum drugs at the molecular level. *Oncol. Rep.* 2003; 10: 1663–1682. DOI: 10.3892/or.10.6.1663
- [188] Andre N, Schmiegel W. Chemoradiotherapy for colorectal cancer. *Gut.* 2005; 54: 1194–1202. DOI: 10.1136/gut.2004.062745
- [189] Sicard-Roselli C, Brun E, Gilles M, Baldacchino G, Kelsey C, McQuaid H, Polin C, Wardlow N, Currell F. A new mechanism for hydroxyl radical production in irradiated nanoparticle solutions. *Small* 2014; 10: 3338–3346. DOI: 10.1002/sml.201400110.
- [190] Coulter JA, Jain S, Forker J, McMahon SJ, Schettino G, Prise KM, Currell FJ, Hirst DG. Evaluation of cytotoxicity and radiation enhancement using 1.9 nm gold particles:

- potential application for cancer therapy. *Nanotechnology*. 2010; 29: 295101. DOI: 10.1088/0957-4484/21/29/295101
- [191] Butterworth KT, Wyer JA, Brennan-Fournet M, Latimer CJ, Shah MB, Currell FJ, Hirst DG. Variation of strand break yield for plasmid DNA irradiated with high-Z metal nanoparticles. *Radiat. Res.* 2008; 170: 381–387. DOI: 10.1667/RR1320.1
- [192] Chang MY, Shiau AL, Chen YH, Chang CJ, Chen HH, Wu CL. Increased apoptotic potential and dose-enhancing effect of gold nanoparticles in combination with single-dose clinical electron beams on tumor-bearing mice. *Cancer Sci.* 2008; 99: 1479–1484. DOI: 10.1111/j.1349-7006.2008.00827.x
- [193] Coulter JA, Hyland WB, Nicol J, Currell FJ. Radiosensitising nanoparticles as novel cancer therapeutics—Pipe dream or realistic prospect? *Clin. Oncol.* 2013; 25: 593–603. DOI: 10.1016/j.clon.2013.06.011
- [194] Hainfeld JF, Slatkin DN, Smilowitz HM. The use of gold nanoparticles to enhance radiotherapy in mice. *Phys. Med. Biol.* 2004; 49: N309–N315. DOI:10.1088/0031-9155/49/18/N03
- [195] Jain S, Coulter JA, Hounsell AR, Butterworth KT, McMahon SJ, Hyland WB, Muir MF, Dickson GR, Prise KM, Currell FJ, O'Sullivan JM, Hirst DG. Cell-specific radiosensitization by gold nanoparticles at megavoltage radiation energies. *Int. J. Radiat. Oncol. Biol. Phys.* 2011; 79: 531–539. DOI: 10.1016/j.ijrobp.2010.08.044
- [196] Chithrani BD, Stewart J, Allen C, Jaffray DA. Intracellular uptake, transport, and processing of nanostructures in cancer cells. *Nanomed.: Nanotechnol. Biol. Med.* 2009; 5: 118–127. DOI: 10.1016/j.nano.2009.01.008
- [197] Chithrani DB. Nanoparticles for improved therapeutics and imaging in cancer therapy. *Recent Patents Nanotechnol.* 2010; 4: 171–180. DOI: 10.2174/187221010792483726
- [198] Chithrani DB. Gold nanoparticles as radiation sensitizers in cancer therapy. *Radiat. Res.* 2010; 173: 719–728. DOI: 10.1667/RR1984.1
- [199] Liu CJ. Enhancement of cell radiation sensitivity by pegylated gold nanoparticles. *Phys. Med. Biol.* 2010; 55: 931–945. DOI: 10.1088/0031-9155/55/4/002
- [200] Hainfeld JF, Slatkin DN, Focella TM, Smilowitz HM. Gold nanoparticles: a new X-ray contrast agent. *Br. J. Radiol.* 2006; 79: 248–253. DOI: 10.1259/bjr/13169882
- [201] Brun E, Duchambon P, Blouquit Y, Keller G, Sanche L, Sicard-Roselli C. Gold nanoparticles enhance the X-ray-induced degradation of human centrin 2 protein. *Radiation Physics and Chemistry.* 2009; 78: 177–183. DOI: 10.1016/j.radphyschem.2008.11.003
- [202] Kang B, Mackey MA, El-Sayed MA. Nuclear targeting of gold nanoparticles in cancer cells induces DNA damage, causing cytokinesis arrest and apoptosis. *J. Am. Chem. Soc.* 2010; 132: 1517–1519. DOI: 10.1021/ja9102698
- [203] Hébert E, Debouttière P-J, Lepage M, Sanche L, Hunting DJ. Preferential tumor accumulation of gold nanoparticles, visualized by magnetic resonance imaging:

radiosensitization studies in vivo and in vitro. *Int. J. Radiat. Biol.* 2010; 86: 692–700. DOI: 10.3109/09553001003746067

- [204] Bobyk L, Edouard M, Deman P, Vautrin M, Pernet-Gallay K, Delaroche J, Adam JF, Estève F, Ravanat JL, Elleaume H. Photoactivation of gold nanoparticles for glioma treatment. *Nanomedicine.* 2013; 9: 1089–1097. DOI: 10.1016/j.nano.2013.04.007
- [205] Hyun Cho S, Jones BL, Krishnan S. The dosimetric feasibility of gold nanoparticle-aided radiation therapy (GNRT) via brachytherapy using low-energy gamma-/x-ray sources. *Phys. Med. Biol.* 2009; 54: 4889–4905. DOI: 10.1088/0031-9155/54/16/004
- [206] Lechtman E, Mashouf S, Chattopadhyay N, Keller BM, Lai P, Cai Z, Reilly RM, Pignol JP. A Monte Carlo-based model of gold nanoparticle radiosensitization accounting for increased radiobiological effectiveness. *Phys. Med. Biol.* 2013; 58: 3075–3085. DOI: 10.1088/0031-9155/58/10/3075
- [207] McMahon SJ, Mendenhall, MH, Jain S, Currell F. Radiotherapy in the presence of contrast agents: a general figure of merit and its application to gold nanoparticles. *Phys. Med. Biol.* 2008; 53: 5635–5651. DOI: 10.1088/0031-9155/53/20/005
- [208] McQuaid HN, Muir MF, Taggart LE, McMahon SJ, Coulter JA, Hyland WB, Jain S, Butterworth KT, Schettino G, Prise KM, Hirst DJ, Botchway SW, Currell FJ. Imaging and radiation effects of gold nanoparticles in tumour cells. *Sci. Rep.* 2016; 6: 19442. DOI: 10.1038/srep19442
- [209] Cho S. Estimation of tumour dose enhancement due to gold nanoparticles during typical radiation treatments: a preliminary Monte Carlo study. *Phys. Med. Biol.* 2005; 50: N163–173. DOI: 10.1088/0031-9155/50/15/N01
- [210] Rahman WN. Enhancement of radiation effects by gold nanoparticles for superficial radiation therapy. *Nanomedicine.* 2009; 5: 136–142. DOI: 10.1016/j.nano.2009.01.014
- [211] Carter JD, Cheng NN, Qu Y, Suarez GD, Guo T. Nanoscale energy deposition by X-ray absorbing nanostructures. *J. Phys. Chem. B.* 2007; 111: 11622–11625. DOI: 10.1021/jp075253u
- [212] Casta R, Champeaux J-P, Moretto-Capelle P, Sence M, Cafarelli P. Electron and photon emissions from gold nanoparticles irradiated by X-ray photons. *J. Nanoparticle Res.* 2015; 17: 1–17. DOI: 10.1007/s11051-014-2807-2
- [213] Casta R, Champeaux JP, Sence M, Moretto-Capelle P, Cafarelli P. Comparison between gold nanoparticle and gold plane electron emissions: a way to identify secondary electron emission. *Phys. Med. Biol.* 2015; 60: 9095–9105. DOI: 10.1088/0031-9155/60/23/9095
- [214] Xiao F, Zheng Y, Cloutier P, He Y, Hunting DJ, Sanche L. On the role of low-energy electrons in the radiosensitization of DNA by gold nanoparticles. *Nanotechnology.* 2011; 22: 465101. DOI: 10.1088/0957-4484/22/46/465101

- [215] Zheng Y, Hunting DJ, Ayotte P, Sanche L. Radiosensitization of DNA by gold nanoparticles irradiated with high-energy electrons. *Radiat. Res.* 2008; 169: 19. DOI: 10.1667/RR1080.1
- [216] Zheng Y, Sanche L. Gold nanoparticles enhance DNA damage induced by anti-cancer drugs and radiation. *Radiat. Res.* 2009; 172: 114–119. DOI: 10.1667/RR1689.1.
- [217] Zheng Y, Cloutier P, Hunting D. J, Sanche L. Radiosensitization by gold nanoparticles: comparison of DNA damage induced by low and high-energy electrons. *J. Biomed. Nanotechnol.* 2008; 4: 469–473. DOI: 10.1166/jbn.2008.012
- [218] Yao X, Huang C, Chen X, Zheng Y, Sanche L. Chemical radiosensitivity of DNA induced by gold nanoparticles. *J. Biomed. Nanotechnol.* 2015; 11: 478–485. DOI: 10.1166/jbn.2015.1922
- [219] Sanche L. Cancer treatment: low-energy electron therapy. *Nat. Mater.* 2015; 14: 861–863. DOI: 10.1038/nmat4333
- [220] Shi M, Thippayamontri T, Gendron L, Guérin B, Paquette B, Sanche L. Increased radiosensitivity of colorectal tumor with intra-tumoral injection of low dose of gold nanoparticles. (in press).